CHALMERS
UNIVERSITY OF TECHNOLOGY

System-level simulations of the effects of driving cycles and driver behavior on the energy flow in a battery electric vehicle

Master´s thesis in Automotive Engineering

Bernd Grohmann

Department of Mechanics and Maritime Sciences

Vehicle Engineering and Autonomous Systems
CHALMERS UNIVERSITY OF TECHNOLOGY
Gothenburg, Sweden 2020

Master´s Thesis 2020:66

System-level simulations of the effects of driving cycles and driver behavior on the energy flow in a battery electric vehicle

Bernd Grohmann

CHALMERS
UNIVERSITY OF TECHNOLOGY

Department of Mechanics and Maritime Sciences
Division of Vehicle Engineering and Autonomous Systems
Chalmers University of Technology
Gothenburg, Sweden 2020

System-level simulations of the effects of driving cycles and driver behavior on the energy flow in a battery electric vehicle
Bernd Grohmann

Supervisor: Docent Jelena Andric, Vehicle Engineering and Autonomous Systems (VEAS), Chalmers
Industrial co-supervisor: Dr. Gunnar Latz, Siemens Industry Software AB
Examiner 1: Prof.Dr.-Ing. Georgios Bikas, Nuremberg Institute of Technology
Examiner 2: Prof.Dr.-Ing. Ulrich Grau, Nuremberg Institute of Technology
Examiner 3: Docent Jelena Andric, VEAS, Chalmers

Master's Thesis 2020:66
Department of Mechanics and Maritime Sciences
Division of Vehicle Engineering and Autonomous Systems
Chalmers University of Technology
SE-412 96 Gothenburg
Telephone +46 31 772 1000

Typeset in LaTeX
Gothenburg, Sweden 2020

System-level simulations of the effects of driving cycles and driver behavior on the energy flow in a battery electric vehicle

Bernd Grohmann
Department of Mechanics and Maritime Sciences
Division of Vehicle Engineering and Autonomous Systems
Chalmers University of Technology

Abstract

Fully-electric car technology has made enormous progress in recent years. With driving range as one of the key factors for commercial success and the vast variety of real-world driving behaviour, the question arises how different levels of driving aggressiveness and drive cycles influence the energy flow in a Battery Electric Vehicle (BEV). Vehicle-level simulations in Siemens Simcenter Amesim were carried out to assess the energy flow in the BEV. Both standard drive cycles and real-world drive patterns represented city, rural and highway driving were considered. The driving aggressiveness was modelled by considering velocity modified and acceleration modified drive patterns separately. The simulation results show that drive cycles with high RPA and relatively low average velocity (20-30 km/h) have the lowest energy consumption due to the ability of BEVs to recuperate energy from regenerative braking and their high average efficiency at these velocities. Thus, BEVs are more sensitive to changes in velocities than in accelerations. High accelerations not only increase the inertia work share of the drive cycle, but also the amount of energy recuperated by regenerative braking. Higher velocities, however, only increase the road work part of wheel work leading to increase in energy demand without the possibility to recover it through regenerative braking. Although questions such as the exact impact of road slopes on energy consumption remain open to further investigation, it can be stated that BEVs are particularly suitable for city traffic with its frequent braking events and relatively low average velocities.

Keywords: BEV, Drive Cycle, Energy Flow, Simulation, Driving Aggressiveness, Driving Behavior

Acknowledgements

Throughout the work on this thesis, I have received a great deal of support and help.

First of all I would like to thank my supervisor, Docent Jelena Andric, whose expertise was invaluable in developing the methodology and results of the thesis. Her feedback has helped me to sharpen my understanding of the research topic and elevated my scientific working to a higher level.

I would like to thank Prof. Georgios Bikas from TH-Nürnberg for enabling me to write my Master's thesis at Chalmers University of Technology. This thesis would never have been possible without his research collaboration with Jelena.

I would also like to thank my co-supervisor Dr. Gunnar Latz from Siemens Industry Software AB for his valuable support and advice regarding the simulation software. Likewise, I would like to thank Siemens Industry Software AB and Chalmers for providing me access to the simulation software Siemens Simcenter Amesim.

In addition, I would also like to thank the entire staff of the Division of Vehicle Engineering and Autonomous Systems for my wonderful time at Chalmers. In particular, I would like to thank Sonja Laakso Gustafsson who supported me in administrative matters. I am also grateful to Dr. Majid Astaneh for the exchange of ideas about the thesis topic and his expertise in the field of battery technology.

Finally, I would like to thank my family for their support during my studies, without whom I could not have done this thesis.

Bernd Grohmann, Nürnberg, September 2020

Contents

List of Figures

List of Tables

1
Introduction

1.1 Motiviation

Fully-electric car technology has made enormous progress in recent years. With more than 1 million Battery Electric Vehicle BEV sold worldwide in 2017, global sales increased 54 % compared to the previous year [12]. Various political and economical factors have an impact on this trend which can be related to megatrends. Those trends describe long-term transformation processes, containing concerns for energy security, air pollution and climate change legislation, support for industrial competitiveness, recent technology improvements, and growing interest for electromobility in key markets such as China [6].
The advantages of BEV´s, compared to conventional vehicles, are their low pollution emission, fast speed response, low noise and high driving efficiency. However, with electricity as propulsion energy,BEV depend solely on batteries as their on-board energy storage device, making cruising range of electric vehicles limited by battery capacity and power density. In combination with a charging station grid that does not yet cover the requirements needed, range anxiety becomes a real hurdle for BEV acceptance. One way in reducing range anxiety is being able to accurately and reliably predict driving range, which is not only dependant on vehicle parameters but also on the driven route and driver behaviour [13].

1.2 Purpose of the thesis and contribution

The overall aim if this thesis is to investigate the effects of driving cycles and driving behaviour on the energy flow in BEVs which can be divided into the following subsections.

- Vehicle parameters for a BEV model were first determined to make it possible for the vehicle to follow various drive cycles for different levels of driving aggressiveness. The BEV model with these parameters was then used for all simulations within this work.
- Modified drive cycles with different levels of driving aggressiveness were created and the simulation results were compared to analyse how the BEV models output parameters were influenced, following the modified drive cycles. The parameters of interest were: energy consumption, regenerative braking, average overall efficiency and wheel work.
- The sensitivity of energy consumption to wheel work was quantified using the definition of the sensitivity from [11].

- Logged real-world driving patterns [1] were used to compare the results found.

1.3 Previous research

The present thesis focuses on BEVs and builds further on the previous work for conventional vehicles as summarized below.

Ref. [2] Analyses the effects of driving style and vehicle performance on the real world fuel consumption of conventional vehicles by using vehicle simulation to assess the sensitivity of fuel consumption to a wide range of driving patterns. The methodology of this study was used as a framework for assessing the energy flow in the BEV in Chapter 5.

Ref. [11] quantified the impact of main component parameters to sensitivity for conventional and hybrid vehicles, by introducing a definition for sensitivity, which allows for comparison between different drive cycles. This definition is utilized in Chapter 6.

Ref. [7] studied and characterized various legislative and real-world drive cycles in terms of speed and acceleration cycles parameters, as well as speed and acceleration distribution. The same way of categorizing drive cycles in city, rural and highway driving is used and explained in Chapter 2.

1.4 Methodology

Siemens Simcenter Amesim system-level simulation software was used to create a BEV model, which is described in Chapter 4. A cooperation between Siemens and Chalmers existed within the scope of this work regarding software support and implementation.

Besides vehicle simulations, vehicle dynamics are utilized to assess the vehicle energy usage. Chapter 3 presents the required equations and explains how they are calculated and interpreted.

Three different standard drive cycles each for city, rural and highway driving are used to simulate different types of driving behavior. Beside the standard drive cycles, we utilized logged real-world drive patterns driven in and around Göteborg. Chapter 2 presents the used standard drive cycles and real-world drive patterns. Driver behavior is modelled through various level of driving aggressiveness in two different ways, shown in Section 2.1.

Chapter 5 discusses the energy consumption for the modified standard cycles showing various BEV-output parameters versus either average velocity or average positive acceleration.

The sensitivity of energy consumption to wheel work is quantified in Chapter 6.

Chapter 7 examines the behavior of the logged drive patterns relative to each other and in comparison to the standard drive cycles.

2
Drive cycle dynamics

This section provides a brief overview over the used standard drive cylces and logged drive patterns. It explains how the cycles were classified and for which purpose they were developed [5][9].

2.1 Drive cycles

Drive cycles consisting of standardized speed profiles were developed to provide a uniform test procedure for comparing vehicle parameters, such as pollutant emissions and fuel consumption. Nowadays, vehicles operate in various environments, are used by different types of drivers and for a wide range of applications. Each of these circumstances has its specific requirements for the vehicle in regard to static and dynamic road load. Accordingly, there are several common standardized drive cycles representing a specific type of driving.

In [1], it is proposed to group drive cycle according to the categories city, rural and highway based, on their share of time spent at different speed levels. City driving is defined as speed below 60 km/h, rural driving between 60-90 km/h and highway driving above 90 km/h. This categorization is adopted for the rest of the thesis.

From the velocity data some parameter can be derived, which are usually used to describe characteristics of drive cycles. Table 2.1 lists: duration, distance, maximum velocity, average velocity, average positive acceleration, RPA and idling. Section 4.3 explains these parameters.
The power required by an engine to accelerate a vehicle depends on both velocity and acceleration, so a combination of the two provides a useful measure of the load an engine is placed on during acceleration. The combined parameter Relative Positive Acceleration (RPA) is calculated by Formula 2.1,

$$RPA = \frac{\int (v * a_{pos})\, dt}{\int v\ dt} \tag{2.1}$$

where v is the current vehicle velocity and a_{pos} the current positive acceleration. Since RPA is distance normalized, it can be compared over drive cycles of varying length. Drive Cycles with RPA values of less than 0.10 m/s^2 are seen as "soft", which typically applies to highway cycles with few and light accelerations. Drive cycles with RPA values greater than 0.20 m/s^2 are considered more aggressive. Typically cycles with rapid accelerations and low velocities have the highest RPA values.

2.1.1 Standard drive cycles

The New York City Cycle **NYCC** was developed in 1975 by the New York City Department of Environmental Protection (DEP). With a travel distance of 1897 m, an average velocity of 12 km/h and an idling period of 39 % of the total time, NYCC represents highly congested urban driving.
Due to lack the of non urban fuel economics in 1974, DAE developed the Highway Fuel Economy Test **HWFET** drive cycle. HWFET represents interstate highway and rural driving. The Driving distance is 16.605 km with an average velocity of 78 km/h. After a steep acceleration at the beginning, the vehicle speed is constantly maintained above values of 70 km/h.
The California Unified cycle **LA92** was developed in 1992 by the California Air Resources Board (CARB). The cycle represents aggressive rural driving over a driving range of 15.8 km, an average velocity of 40 km/h with a maximum speed of 108 km/h and an idling period of 11 % of the total time.
The **US06** drive cycle merged high-speed driving with an average velocity of 78 km/h, with high-acceleration driving of 0.31 m/s^2 due to his rapid speed fluctuations.
The non legislative drive cycles **ArtemisURBAN, ArtemisRURAL** and **ArtemisHW130** were developed within the European Artemis research projekt. All three cycles have a driving time of approximately 1000 s and were developed from real world driving data obtained from 77 instrumented vehicles tracked for 2000 days in France, UK, Germany and Greece.
Most recently the **WLTC class 3-2** (Worldwide harmonized) was developed to have a worldwide acceptable standard drive cycle for vehicles with power to mass ratio greater than 34 W/kg and a higher maximum velocity than 120 km/h. It consists of four driving segments, low, medium, high and extra high. In order to correspond to the previously introduced categorization of drive cycles, only the low and high segments are used as standard drive cycles. **WLTClow** for city driving and **WLTChigh** for rural driving, respectively. Driving parameters derived from the drive cycles are presented in Table 2.1

Table 2.1: Drive cycle characteristics for standard drive cycles.

	Duration [s]	Distance [m]	Max Velocity [km/h]	Average Velocity [km/h]	Aver. pos. Accel. [m/s^2]	Idling [%]	RPA [m/s^2]
NYCC	598	1 897	45	12	0.21	39	0.32
ArtemisURBAN	993	4 871	58	18	0.28	25	0.32
WLTClow	588	3 095	56	19	0.17	30	0.21
LA92	1435	15 799	108	40	0.26	11	0.23
WLTChigh	455	7 124	97	56	0.17	11	0.12
ArtemisRURAL	1082	17 273	112	57	0.21	1	0.18
US06	596	12 888	129	78	0.31	6	0.21
ArtemisHW130	1068	28 736	132	97	0.18	0.8	0.14
HWFET	765	16 506	96	78	0.09	0.5	0.07

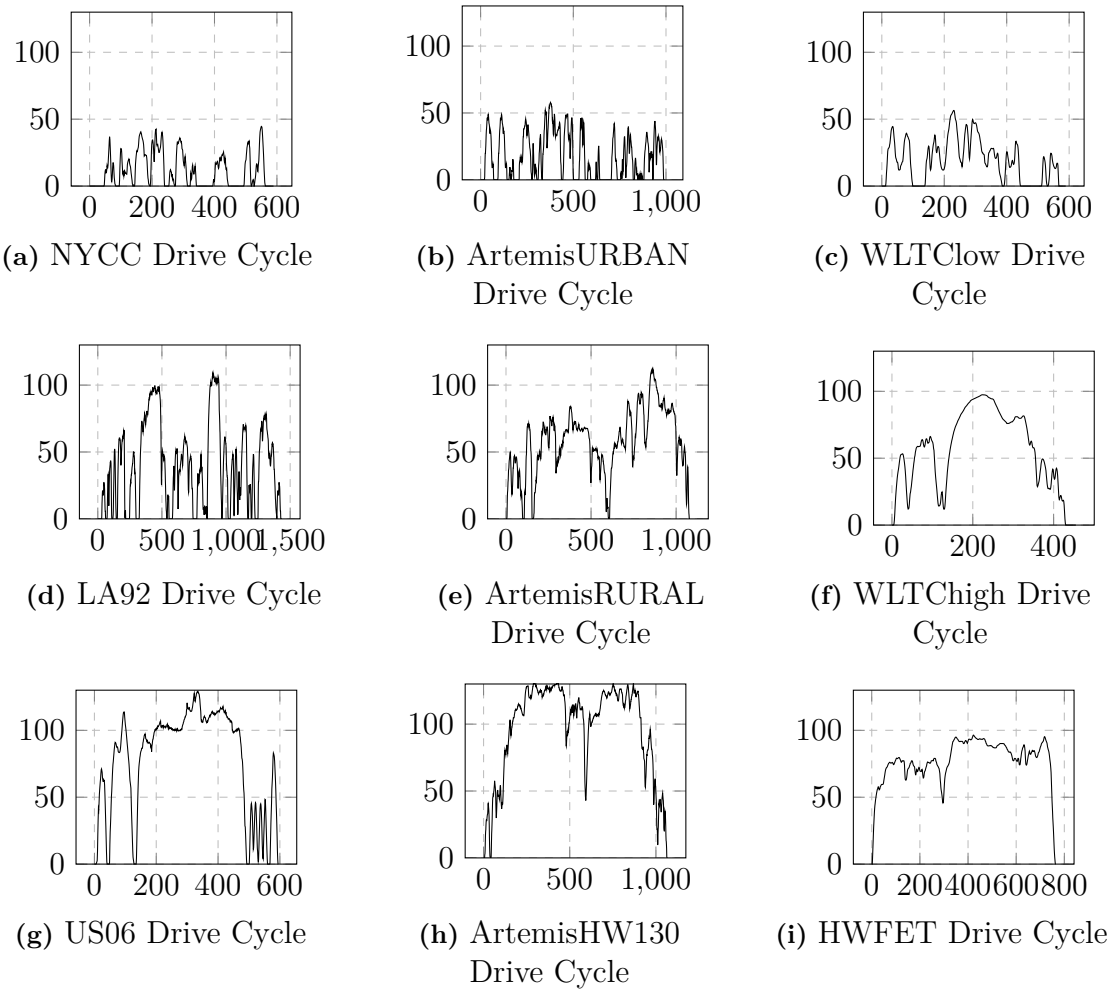

(a) NYCC Drive Cycle

(b) ArtemisURBAN Drive Cycle

(c) WLTClow Drive Cycle

(d) LA92 Drive Cycle

(e) ArtemisRURAL Drive Cycle

(f) WLTChigh Drive Cycle

(g) US06 Drive Cycle

(h) ArtemisHW130 Drive Cycle

(i) HWFET Drive Cycle

Figure 2.1: Overview of the standard drive cycles

2.1.2 Logged drive patterns

In addition to standard drive cycles, logged drive patterns created with a GPD-accelerometer measurement system were used. For detailed information on how the logged cycles were recorded, see [1]. This data was collected within the Division of Electric Power Engineering at Chalmers University of Technology and consists of nine low-speed routes (LS1-LS9), five middle-speed routes (MS1-MS5) and two high-speed routes (HS1-HS2). Some routes have been recorded in both directions such as HS1 A-B and HS1 B-A. Velocity and vehicle altitude plots for logged cycles can be seen in Appendix A.

Table 2.2: Drive cycle characteristics for logged drive patterns.

	Duration [s]	Distance [m]	Max Velocity [km/h]	Average Velocity [km/h]	Average pos. Acceleration [m/s²]	Idling time [%]	RPA [m/s²]
HS 1 AtoB	3080	54 225	115	63	0.16	0.8	0.13
HS 1 BtoA	2309	51 030	125	80	0.16	0.04	0.13
HS 2 AtoB	7075	149 411	114	76	0.11	1.5	0.08
HS 2 BtoA	6576	149 454	118	82	0.10	0.03	0.07
MS 1 AtoB	1141	14346	110	45	0.22	0.3	0.21
MS 1 BtoA	1340	13725	84	37	0.22	0.1	0.21
MS 2 AtoB	1696	30540	100	65	0.16	0.002	0.15
MS 2 BtoA	1684	30926	125	66	0.23	0.07	0.24
MS 3	2046	30557	113	54	0.24	0.2	0.20
MS 4	1178	13899	85	42	0.21	1.5	0.19
MS 5a	716	7572	90	38	0.23	0.5	0.22
MS 5b	529	7190	83	49	0.23	0.08	0.22
MS 5c	534	7162	83	48	0.31	2.7	0.29
LS 1	2633	12921	60	18	0.24	1.8	0.28
LS 2	1558	13125	74	30	0.25	1.1	0.23
LS 3	826	4958	48	22	0.25	0.3	0.24
LS 4 AtoB	790	9096	67	41	0.21	0.1	0.20
LS 4 BtoA	866	9771	76	41	0.25	0.07	0.22
LS 5	1038	11582	78	40	0.21	0.04	0.19
LS 6	1437	7451	68	19	0.23	1.9	0.26
LS 7	365	1607	50	16	0.30	1.2	0.38
LS 8 AtoB	694	7760	67	40	0.23	0.6	0.22
LS 8 BtoA	806	7930	64	35	0.22	0.7	0.21
LS 9	1213	5243	53	16	0.23	1.7	0.28

2.2 Driving behavior

This section explains how driving behavior is modelled. An artificial aggressiveness factor k was used to model different levels of driving aggressiveness and therefore driving behavior. The introduction of an artificial parameter is particularly useful because it creates a consistent measure by which aggressiveness of a cycle can be manipulated [11].
The most common way of modelling driving behavior is the trace modifier. Here, only the speed trace is multiplied by k, resulting in a scaling of velocity and acceleration of the drive cycle, as shown in Figure 2.2.

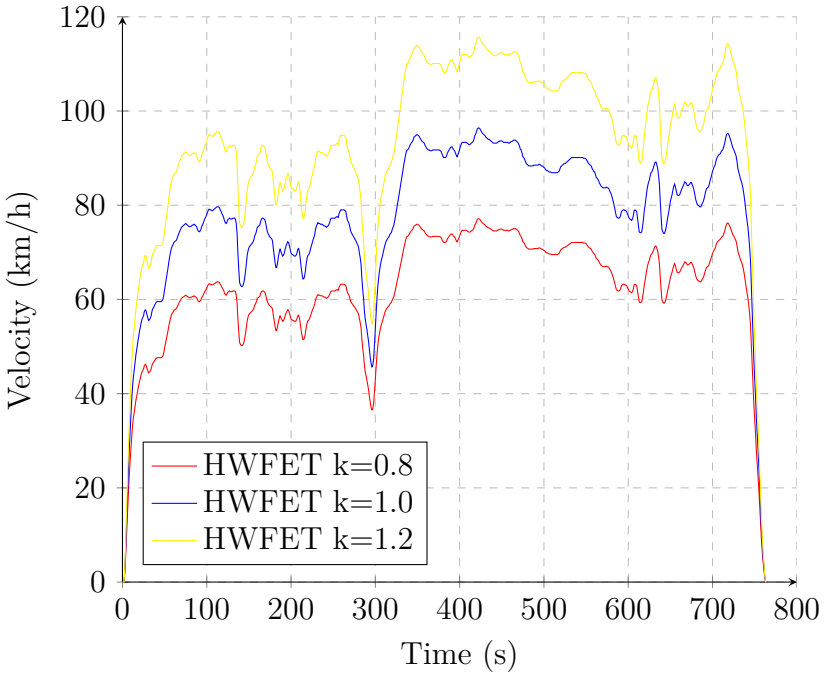

Figure 2.2: Trace modified drive cycle

It is beneficial to study the influence of velocity and acceleration separately by scaling only one variable while the other remains constant. Velocity is scaled by multiplying both velocity and time with the factor k, as it is shown in Figure 2.3. The cycle then reaches higher velocities over a longer time and distance, so that the acceleration remains constant. As a consequence, however, the acceleration now occurs at higher velocity levels. Acceleration is scaled by multiplying only time with the aggressiveness factor, as seen in Figure 2.4. This also changes the duration time it takes to reach the same velocity [8].

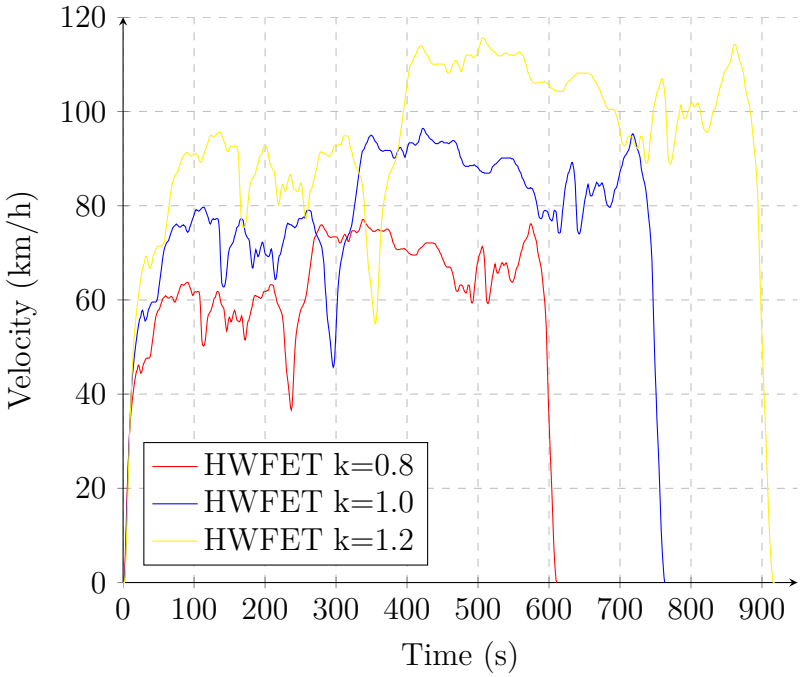

Figure 2.3: Velocity modified drive cycle

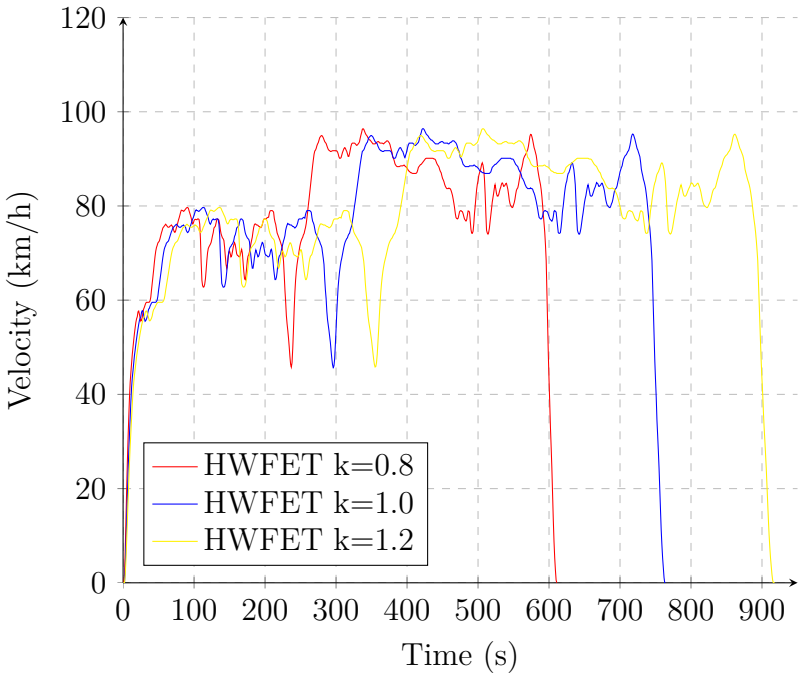

Figure 2.4: Acceleration modified drive cycle

3

Vehicle dynamic

The following section introduces dynamic variables of drive cycle, such as tractive force, tractive power and wheel work, which are useful to evaluate and understand the energy flow in the BEV model. It describes how these variables are calculated from velocity, acceleration and vehicle parameters so that we can later investigate how velocity and acceleration affects energy consumption.

While driving a vehicle, two fundamental effects occur.

1. Mechanical energy generated by the propulsion system is presumed to be temporarily stored in the vehicle.
2. Energy is withdrawn from this energy storage system through dissipative processes.

Part of the systems exergy is transformed into anergy through dissipating due to three main effects.

Aerodynamic friction losses

A vehicle in motion experiences aerodynamic resistance F_a due to two main causes. First, viscous friction from the surrounding air acts on the surface of the vehicle and second, the losses resulting of pressure differences between the front and rear of the vehicle, created by a separation of the air flow. This pressure field can be calculated using numerical methods for idealized vehicles shapes. However, determining the influence of particular effects is only possible with specific measurements in wind tunnels. In the literature the aerodynamic force is often approximated by simplifying the vehicle as a prismatic body. The aerodynamic resistance of the simplified model is expressed as,

$$F_a = \frac{1}{2} * \rho_{air} * A_f * c_d * v^2 \tag{3.1}$$

where ρ_{air} $(\frac{\text{kg}}{\text{m}})$ is the ambient air density, A_f (m^2) the frontal vehicle area, v $(\frac{m}{s})$ the vehicle velocity and c_d the aerodynamic drag coefficient, which models the actual flow conditions. The coefficient c_d $(-)$ depends on multiple parameters, such as flow velocity, fluid density, fluid viscosity and others. However, the value c_d is assumed to be constant in this thesis.
Since the specification of a drag coefficient only makes sense together with the corresponding reference frontal area, the parameter drag area $c_d A_f$ is often found in the literature.

Rolling friction losses

The rolling friction resistance F_r of a vehicle can be modelled as,

$$F_r = c_r * m_v * g * cos(\alpha) \tag{3.2}$$

with c_r as friction coefficient, m_v (kg) as vehicle mass, g ($\frac{m}{s^2}$) as acceleration due to gravity and α (rad) as road inclination angle. $cos(\alpha)$ is usually negligible in practice, and since standard drive cycles normally do not contain any information about road inclination, we neglect the influence of the parameter. The friction coefficient depends on the vehicle speed, tire pressure and profile as well as road surface conditions. Since the friction coefficient changes only slightly when driving moderate velocities, it is assumed to be constant for this study.

Grade resistance

A vehicle driving on a non-horizontal road experiences a force induced by gravity. This grade resistance force F_g has a significant influence on the vehicle performance and can be modelled by the following equation.

$$F_g = m_v * g * sin(\alpha) \tag{3.3}$$

In contrast to the previous terms, grade resistance is not a loss but a storage of potential energy that can either support or hinder the movement of the vehicle. During uphill driving, grade resistance is negative and hinders the movement of the vehicle. When driving downhill, grade resistance is positive and supports the movement of the vehicle.

3.1 Tractive force

According to the Newton´s second law of motion, the acceleration and thus the inertia of an object changes according to the sum of all forces acting on it. The equation for the lateral dynamic motion of a rigid vehicle can be formulated as followed.

$$m_v * a = F_t - (F_a + F_r + F_g) \tag{3.4}$$

Rearranging the formula yields the main equation for calculating the tractive force, which is the force required on the wheels while driving.

$$F_t = \left(\frac{\rho * A_f * c_d * v^2}{2}\right) + (c_r * m_v * g) + (m_v * g * sin(\alpha)) + (m_v * a * \delta) \tag{3.5}$$

The mass correlation factor δ in the inertia term, with the assumed value of 1.04 was added due to the fact that the 4 vehicle wheels must be accelerated both angularly and linearly.
Summarizing only the expressions of aerodynamic friction and rolling friction in Equation 3.5, yields road force $F(v)_{road}$, i.e. the force the vehicle experiences during steady-speed driving without road gradients and excluding all inertia forces $F(a)_{inertia}$.

$$F_t = F(v)_{road} + F(a)_{inertia} \tag{3.6}$$

Depending on the tractive force F_t, three different operation modes for the vehicle can be separated.

- $F_t > 0$ **Traction mode**: The propulsion system provides a driving force and the vehicle either accelerates or drives at steady-speed, when all inertia terms are zero.
- $F_t < 0$ **Braking mode**: The brakes dissipate kinetic energy from the vehicle leading to a decelerating. The inertia force is negative and, in absolute terms, greater than the road force.
- $F_t = 0$ **Coasting mode**: The decreasing kinetic energy matches the resistance losses of the vehicle. Here inertia forces are negative and in absolute numbers equal to road forces.

3.2 Tractive power

Multiplying tractive force by vehicle velocity yields the tractive power that the powertrain has to deliver in order to maintain a certain velocity level.

$$P_t = F_t * v \tag{3.7}$$

The vehicle receives tractive power from the propulsion system only during time spent in traction mode, hence the energy required to follow a drive cycle is described in terms of positive power.

$$P_t = P(v)_{road} + P(a)_{inertia} \tag{3.8}$$

Tractive power can be also divided into velocity and acceleration components, namely road power $P(v)_{road}$ and inertia power $P(a)_{inertia}$.
Road load, consists of aerodynamic and rolling resistance and is always positive. Inerita load consists of grade resistance and inertia and is either negative or positive. The BEV can only recuperate energy during times when the inertia power is negative and in absolute terms greater than the road load. Excess energy can then be used for regenerative braking.

3.3 Wheel work

There are different possibilities to define the energy required to complete a driving cycle like wheel energy, used in [1]. Wheel work was chosen here because it allows a direct comparison of the results of the study [2].

Wheel work expresses the positive energy that is required at the wheels per unit distance. It is calculated by the sum of tractive power when traction power is positive and divided by total distance travelled.

$$W_{wheel} = \frac{\int (P)^{P>0}\, dt}{\int v dt} \tag{3.9}$$

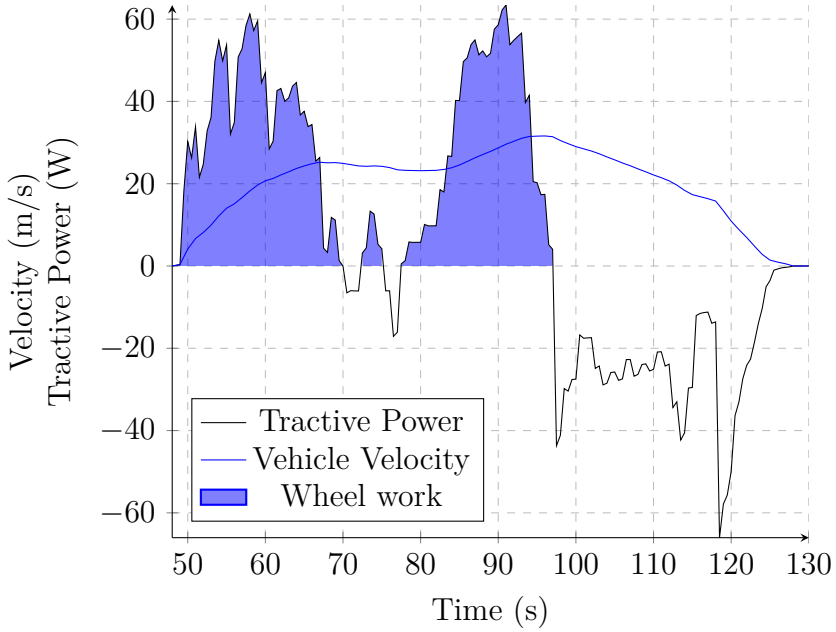

Figure 3.1: Tractive power and velocity for 82 seconds of US06 standard drive cycle

Unlike tractive power, wheel work is always positive because wheel work is tractive power cumulated only when total power is positive, as illustrated in Figure 3.1. Wheel work can be further split into road work $W(v)_{road}$ and inertia work $W(a)_{inertia}$, containing velocity and acceleration components.

$$W_{wheel} = W(v)_{road} + W(a)_{inertia} \tag{3.10}$$

Inertia work is defined as inertia power summed up only when tractive power is negative and divided by total distance travelled. Note that negative inertia power values are also added up for times when tractive power is positive.

$$W_{Inertia} = \frac{\int (P_{Inertia})^{P>0}\, dt}{\int v dt} \tag{3.11}$$

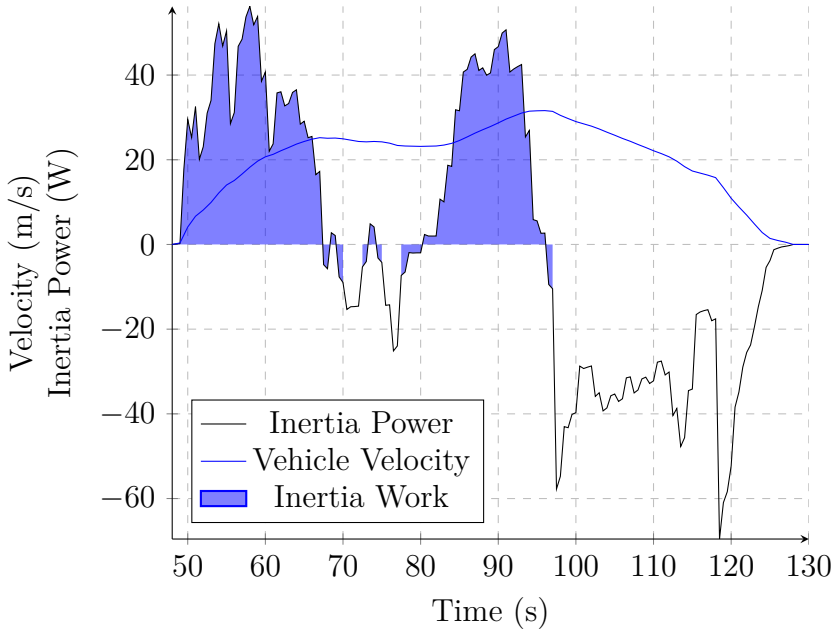

Figure 3.2: Inertia power and velocity for 82 seconds of US06 standard drive cycle

Road work is defined as road power summed up only when tractive power is negative and divided by total distance travelled.

$$W_{Road} = \frac{\int (P_{Road})^{P>0}\, dt}{\int v dt} \tag{3.12}$$

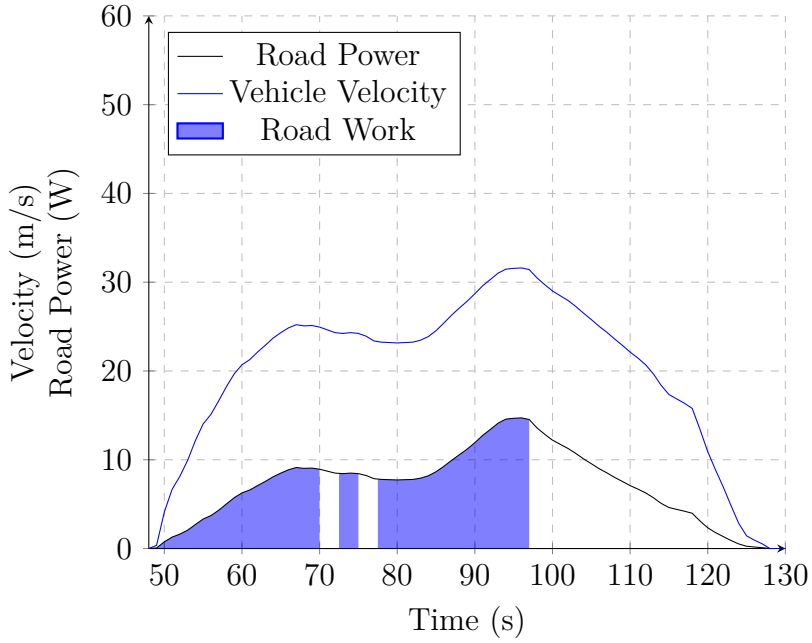

Figure 3.3: Road power and velocity for 82 seconds of US06 standard drive cycle

4
Software

Within the scope of this thesis, the physical based simulation software Siemens Simcenter Amesim was used to analyse the energy flow in a BEV. In the following chapter the structure and function of the BEV-Model is presented by explaining the principles of the individual components and their interaction [3] [4]. It is worth mentioning that the powertrain components used are quasi-static models. Hence, they are based on operating maps which characterise the components during static operation. In the case of highly dynamic simulations, this can lead to a loss of accuracy. However, such high frequencies are not reached in the present simulation.

4.1 BEV-Model

A simplified structure of the model excluding the VCU-component can be found in Figure 4.1.

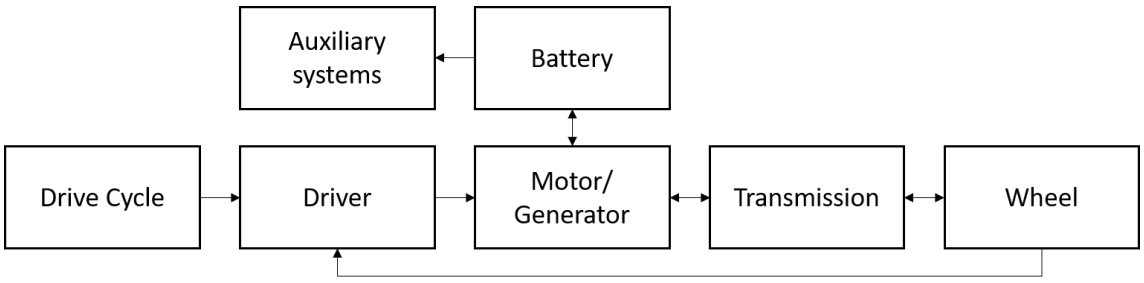

Figure 4.1: Architecture of the BEV-Model

The model shown in Figure 4.2 consists of a pre-existing tutorial model that was modified accordingly. The Driver receives a target velocity from the drive cycle data and sends the driving command to the electric motor. Here the mechanical driving power for the vehicle is computed together with the electrical power output of the battery. The powertrain which includes the battery, electric motor and transmission to wheel can operate bidirectional. Either electrical energy is taken from the battery to propel the vehicle, or regenerative braking is used to convert mechanical braking energy into electrical energy to recuperate the battery.

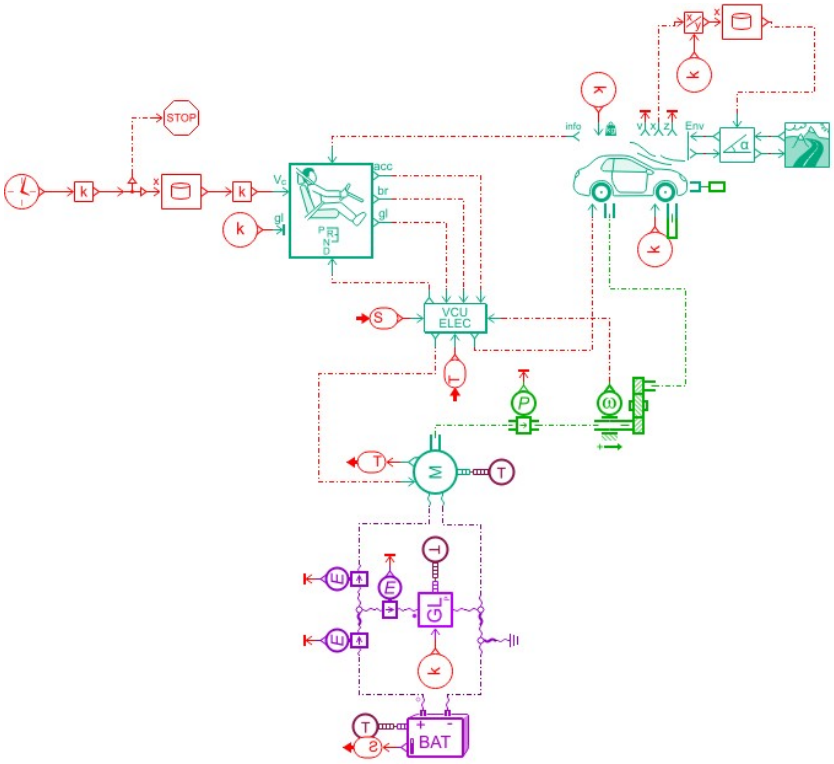

Figure 4.2: Display of the utilized BEV-Model in Siemens Simcenter Amesim

4.1.1 Driver model

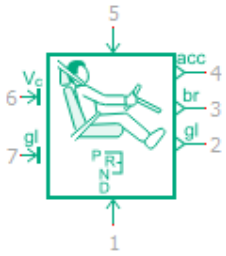

Figure 4.3: Display of the driver component

For this purpose, the longitudinal driver receives data from the vehicle, the powertrain, the environment and the target speed. From the input data, acceleration, brake and gear level commands are computed and sent to the control unit VCU. Figure 4.4 is taken from the Siemens Simcenter Amesim documentation and shows the concepts for computing acceleration and braking command.

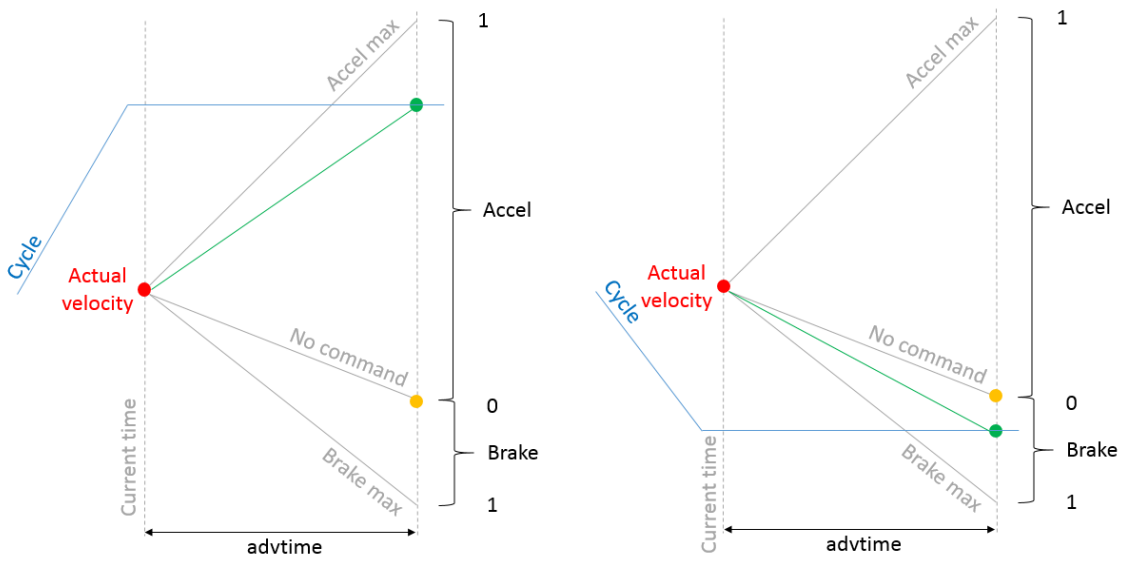

Figure 4.4: Illustration of how Siemens Simcenter Amesim computes the driver commands.

First, the future drive cycle velocity is read in advance (green points) and compared with the future vehicle velocity[1] without command (orange points). Depending on whether the cycle velocity is above or below the future vehicle velocity, the driver must either accelerates or brake and computes the command for both. The "advtime" parameter is the drivers anticipation time. High values means the driver reads the cycle more in advance and his reaction is smother, while low values favour a more responsive and precise behaviour. To ensure that the driver follows the drive cycle closely, the reaction time has been set to 0.01 s.
The driver receives the target velocity in the form of a time velocity 1D table, which has previously been modified with signal components, as shown in figure 4.5.

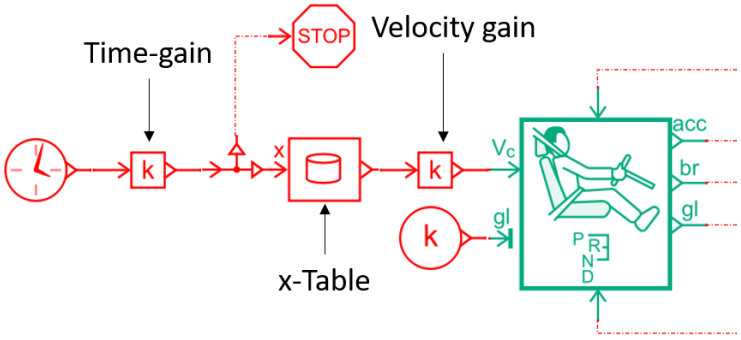

Figure 4.5: Display of the drive cycle modification components.

The dynamic x-table reads the 1D drive cycle files, where the x-column contains the time values in (s) and the y-column the velocity values in $(\frac{m}{s})$. The Velocity gain

[1]The future vehicle velocity is estimated using an internal vehicle model with input parameters from the present vehicle model

component is set to multiply each velocity value with the aggressiveness factor k, scaling the velocity axis of the drive cycle. Independent from this, the time gain component multiplies the simulation time itself. Because time-gain values greater than 1 increase the simulation speed and thereby compress the time axis, inverse values must be used. The stop component causes the simulation to be stopped when the drive cycle is completed.

Unlike standard drive cycles, logged driving patterns have a road inclination file that also needs to be modified. Figure 4.6 shows the necessary component.

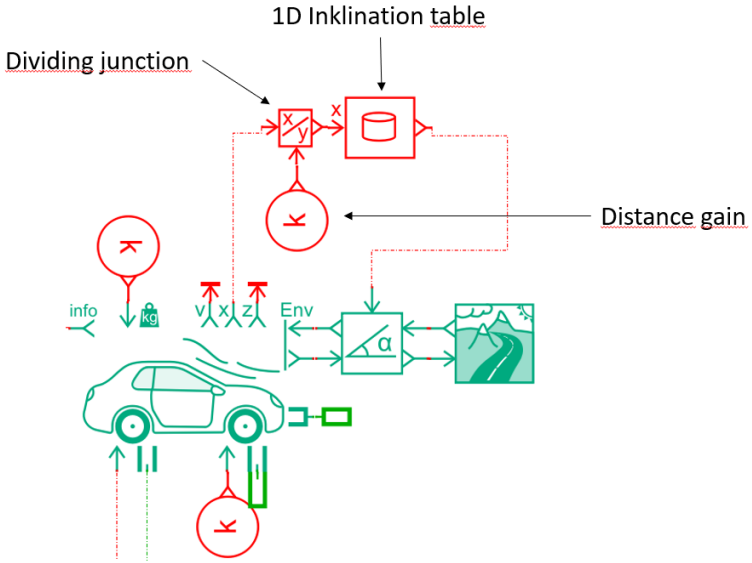

Figure 4.6: Display of the road inclination modification components.

The inclination table reads the road grade in (%) over the vehicle distance in (m). As the distance travelled by the vehicle is changed by velocity or acceleration modifications, the inclination file must be constantly adjusted. This is done by taking the distance travelled directly from the vehicle and dividing it with the distance gain in the component dividing junction.

4.1.2 Vehicle control unit (VCU)

The VCU receives information from the driver, battery and electric motor and analyses the inputs in order to minimize the energy consumption of the battery. From the received acceleration and braking command, it computes the torque asked by the driver, which determines whether the vehicle accelerates or brakes.

- In case of acceleration the positive driving torque is sent to the electric motor.
- In case of braking, the negative braking torque is transmitted either to the electric motor, using regenerative braking for recharging the battery, or to the mechanical vehicle brakes.

In the used simulation model the electric motor torque is mainly used to brake the vehicle. In case of insufficient motor torque available, the vehicle brakes are used

to complete braking. Furthermore, the VCU allows to define a low/high threshold for motor speed and State of Charge (SOC), that defines when regenerative braking is authorized. Both were set accordingly to enable regenerative braking throughout all drive cycles.

4.1.3 Electric motor

This component represents an electric motor/generator model with its converter and can be used bidirectional. It takes the either positive or negative torque T_a (acceleration or braking) from the VCU and determines the output torque to the vehicle T_m. To include the lag time between input and ouput torque, a first-order lag with the time constant $t_s = 0.1\,\mathrm{s}$ is considered in the component.

$$T_m = \frac{1}{1 + t_r * s} * T_a \tag{4.1}$$

Then the mechanical power of the drive shaft P_{mech} is calculated by Formula 4.2.

$$P_{mech} = T_m * \omega \tag{4.2}$$

The angular velocity ω of the motor shaft is defined as negative for forward driving, therefore P_{mech} is negative when propulsion power is delivered to the wheels and positive when tractive power is taken from the wheels.

Electrical power P_{el} is calculated with the help of power lost P_{lost} through Formula 4.3. P_{el} is defined as negative when electrical power is provided to the electric motor and positive when energy is recuperated back into the battery.

$$P_{el} = P_{mech} - P_{lost} \tag{4.3}$$

Values for P_{lost} are read from tables created by the "Electric Motor Tables Creator". The tool generates maps for maximum peak torque, maximum continous torque, power losses and motor efficiency as a function of motor speed, motor torque and voltage, using simple motor data presented in Table 4.1. The motor data is based on a powerful BEV to ensure that the simulation can follow the high acceleration and velocities of the most aggressive drive cycles.

Table 4.1: Characteristics for the electric motor

Motor architecture	squirrel cage asynchronous motor
Continuous base power	360 kW
Max continuous torque	600 Nm
Max speed	23500 rev/min
Nominal Voltage	400 V
Ratio peak	1.01

Two operating modes based on the calculated mechanical and electrical power can be distinguished, as shown in Figure 4.7.

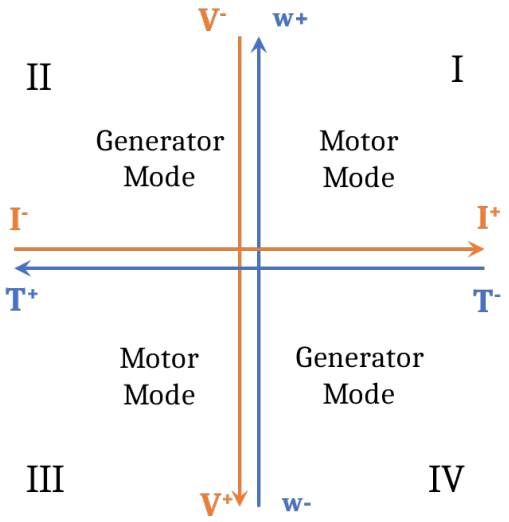

Figure 4.7: Illustration of the electric motor operational modes.

- I: The motor moves **backward** and applies torque that **favours** the movement.
- II: The motor moves **backward** and applies torque that **opposes** the movement.
- III: The motor moves **forward** and applies torque that **favours** the movement.
- IV: The motor moves **forward** and applies torque that **opposes** the movement

The vehicle only moves forward, so the electric motor operates only in the 3 and 4 quadrant. Based on this, the output current I_{out} required by the battery is then defined with the output circuit voltage U_{out} as followed.

$$I_{out} = \frac{P_{el}}{U_{out}} \tag{4.4}$$

4.1.4 Gear

The gear has a single gear ratio α of 10 and a constant efficiency of 95%. It acts as a transition by reducing the rotatory speed while increasing the torque of the drive shaft.

4.1.5 Vehicle model

Figure 4.8: Display of the vehicle component

The vehicle is represented as a simple rigid vehicle load, taken into account the dynamic wheel radius and stictions. In the used configuration "road" road slope, aerodynamic drag, rolling friction forces and climbing resistance are calculated through corresponding vehicle parameters shown in Table 4.2. All equations necessary to calculate the losses the vehicle has to overcome are explained in Chapter 3.

Table 4.2: Characteristics for the electric motor

Vehicle mass m_v	1841 kg
Friction coefficient c_r	0.01
Air penetration coefficient c_d	0.22
Vehicle active are for aerodynamic drag A_f	2.19 m^2
Wheel radius R_{wheel}	0.31 m

The vehicle uses rear wheel propulsion and computes the driving force as followed.

$$F_{dr} = \frac{T_{wheel}}{R_{wheel}} \tag{4.5}$$

Furthermore, the vehicle slip is switched off to ensure a coherent wheel and vehicle velocity.

4.1.6 Auxiliary load

This component accounts for auxiliary systems like air conditioning, power steering, heating or sound system and represents the quasi static behaviour of an automotive load. During simulation the component draws a constant power of 100 W [10].

4.1.7 Battery

The battery model consists of a simple equivalent circuit model with the defining parameters open circuit voltage OCV, internal resistance R and the input current I_{in} leading to a load-dependent input voltage V_{in}. To break potential algebraic loops, a negligible small filtering capacitance $C_f = 10\,\mathrm{F}$ is implemented to the circuit. The physical parameters of the battery correspond to a battery pack, which in turn consists of single cells connected in parallel and in series.

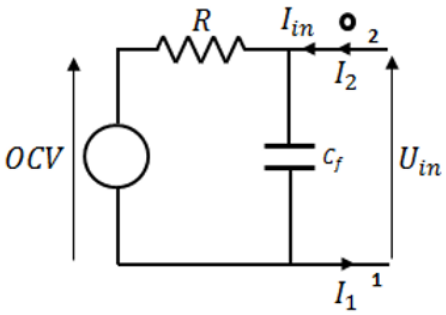

Figure 4.9: Equivalent circuit model of the battery component

The component computes the initial voltage derivative with the help of Kirchhoff´s voltage law.

$$\frac{dU_{in}}{dt} = \frac{I_{in} - \frac{U_{in} - OCV}{R}}{c_f} \tag{4.6}$$

Usually the term state of charge (SOC) is used to indicate how much charge is left in the battery. Its SOC derivative is calculated using the nominal capacitance c_n.

$$\frac{SOC}{dt} = 100\frac{I_{in}}{c_n} \tag{4.7}$$

The nominal capacitance is defined by the energy of the battery pack

$$c_n = \frac{E_{pack}}{OCV} \tag{4.8}$$

and the heat flow dh_b is modelled with the internal resistance Joule losses.

$$dh_b = \frac{(U_{in} - OCV)^2}{R} \tag{4.9}$$

Table 4.3: Characteristics of the electric battery

Open Circuit Voltage OCV	400 V
Internal Resistance R	0.1 Ω
Battery Pack Energy E_{Pack}	75 kW
Filtering Capacity c_f	10 F

4.2 Simulation structure

After discussing the functionality and structure of the BEV-model in the previous sections, this section focuses on how the simulations were prepared and performed. For this purpose, it explains how batch runs are used to modify driving behavior and how the vehicle output parameters were defined and computed using the post processing section.

The main structure can be summarised as followed. Each drive cycle must be modified in terms of velocity and acceleration, as described in Section 2.2. For that purpose, the aggressiveness factor k values between 0.1 and 3.0 with an interval of 0.1, which means that 60 simulations per drive cycle are performed. With the help of the option "Batch run", sequential runs with initiated parameters can be carried out, reducing time and workload. Figure 4.10 shows the design matrices in segments, where velocity and time gain refer to the velocity-gain and time-gain input components described in Figure 4.5.

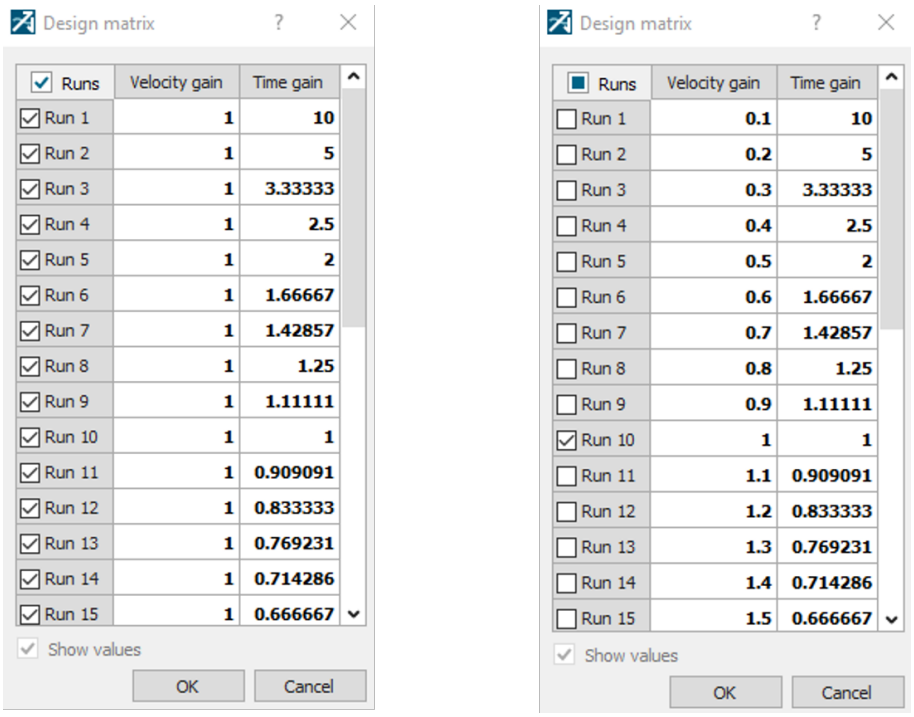

Figure 4.10: Structure of the batch for velocity modified (left) and acceleration modified (right) driving behavior

These batch designs can then be loaded for further drive cycles, whereby only the input for drive cycles and simulation time must be changed once.
Amesim will then successively simulate run 1 to run 30. For the rest of the thesis, these runs are referred to as batches 1 to 30.

4.3 Vehicle output parameters

Component parameters can be linked by mathematical or logical operations in the post-processing area to create new post-processing-parameters. Amesim then calculates these new post-processing-parameters for each executed batch.

Average velocity

The **average velocity** v_a of a drive cycle is defined as velocity summed up and divided by the total simulation time t.

$$v_a = \frac{1}{t} \int v_v \, dt \tag{4.10}$$

Average positive acceleration

The **average positive acceleration** a_a of a drive cycle is the vehicle acceleration a_v summed up and divided by the simulation time only when the acceleration is positive or zero.

$$a_a = \left(\frac{1}{t} \int a_v \, dt \right)^{a_v \geq 0} \tag{4.11}$$

Recuperated energy

Recuperated energy E_{rec} is the amount of energy recuperated from regenerative braking over a drive cycle and is measured at the power sensor directly after the battery. It is calculated by the electric power P_{el} summed up only when the electric power is positive and divided per distance travelled.

$$E_{rec} = \frac{\int (P_{el})^{P_{el}>0} \, dt}{\int v dt} \tag{4.12}$$

Energy consumption

Energy consumption E_{con} is the amount of energy drained from the battery minus the amount of energy recuperated by regenerative braking over a drive cycle. Like E_{rec}, it is measured at the power sensor directly after the battery. It is calculated by the electric power P_{el} summed up only when electric power is negative and divided per distance travelled.

$$E_{con} = \frac{\int (P_{el})^{P_{el}<0} \, dt}{\int v dt} \tag{4.13}$$

Average overall efficiency

Average overall efficiency η_{total} of the BEV model is calculated by multiplying the average efficiency of the battery, electric motor and gear.
The **battery efficiency** η_b is defined as,

$$\eta_b = \frac{useful\ energy}{invested\ energy} = \frac{E_{b,dis}}{E_{b,dis} + E_{loss}} \tag{4.14}$$

where $E_{b,dis}$ is the energy discharged from battery and the heat loss E_{loss} is the cumulative summed heat flow of the battery. In this definition, recuperated energy is not considered useful energy. It is true that recuperated energy is useful for extending the driving range of the vehicle, but it is not useful for the battery itself. In fact the opposite is true. Due to additional heat losses during the recharging process, the battery efficiency is lower with regenerative braking activated than without it.
The constant **gear efficiency** η_{gear} is taken directly as component parameter.
When calculating the **electric motor efficiency** η_{em}, first the efficiencies during motor η_m and generator mode η_g are determined and multiplied with the time shared δ in which each operation mode is active before they are added together.

$$\eta_{em} = \eta_m * \delta_m + \eta_g * \delta_g \tag{4.15}$$

Figure 4.7 shows that the electric motor component is in motor mode while the torque is positive and in generator mode while the torque is negative. Based on this knowledge, both efficiencies of the electric motor can be calculated with the help of corresponding power sensors using the following equations

$$\eta_m = \frac{\int (P_{mech})^{T_m>0}\ dt}{\int (P_{el})^{T_m>0}\ dt} \tag{4.16}$$

and

$$\eta_g = \frac{\int (P_{mech})^{T_m<0}\ dt}{\int (P_{el})^{T_m<0}\ dt} \tag{4.17}$$

The time when the motor mode is active t_m can be calculated by summing up simulation time t when the electric motor torque is positive, divided by the total simulation time times two. The same has been done with the negative torque for the time when the generator mode t_g is active.

$$t_m = \frac{\int (t)^{T>0}\ dt}{\int t\ dt} * 2 \qquad t_g = \frac{\int (t)^{T<0}\ dt}{\int t\ dt} * 2 \tag{4.18}$$

Now the time share in which the motor mode δ_m and generator mode δ_g is active can be computed.

$$\delta_m = \frac{t_m}{t_m + t_g} \qquad \delta_g = \frac{t_g}{t_m + t_g} \tag{4.19}$$

Wheel work

$$W_{wheel} = \frac{\int \left(P(v)_{road} + P(a)_{inertia}\right)^{P>0} dt}{\int v dt} \tag{4.20}$$

The individual parameters for wheel work are described in Chapter 2.

4.4 How batches are plotted

Each batch represents the simulation of a single drive cycle. By plotting the created post-processing parameters for each batch, plots are created that show the driving behavior for different levels of driving aggressiveness, as shown in Figure 4.11.

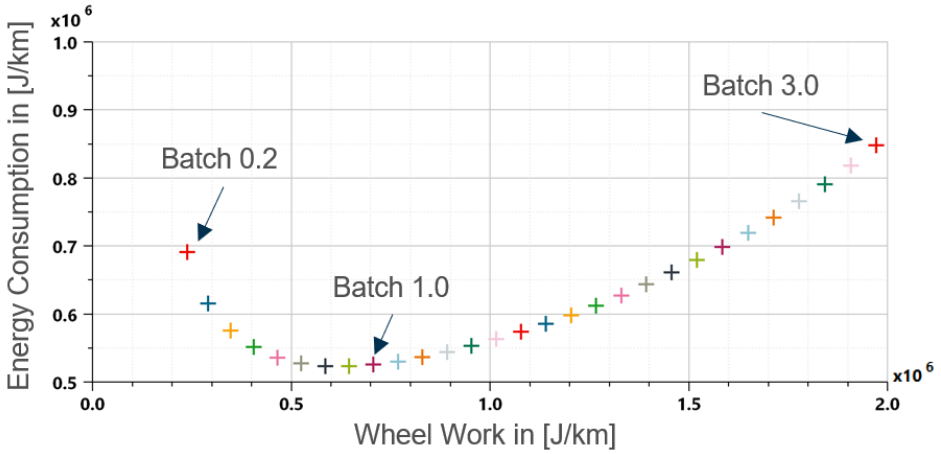

Figure 4.11: Representation of how batches are plotted using energy consumption versus wheel work for velocity modified driving behavior

The BEV-model does not follow the target velocity for every level of driving aggressiveness. Either accelerations become too strong or velocity becomes too high. As a result, it was not always possible to use all 30 batches per drive cycle. Table 4.4 shows which batches were selected for which drive cycle.

Table 4.4: Table of the used batches.

	Velocity modified	Acceleration modified
NYCC	2-30	4-30
ArtemisURBAN	3-30	5-30
WLTClow	2-30	4-30
LA92	2-25	6-30
WLTChigh	1-28	3-30
ArtemisRURAL	1-24	5-30
US06	2-20	4-30
ArtemisHW130	2-21	4-30
HWFET	1-28	3-30
LS2	2-30	4-30
LS4 AtoB	2.30	3-30
LS9	3-30	4-30
MS1 AtoB	2-22	4-30
MS2 AtoB	3-26	4-30
MS3	2-25	4.30
HS1 AtoB	2.24	4-30
HS2 AtoB	2-24	4-30
HS2 BtoA	2-24	4-30

5

How different drive cycles and driving aggressiveness influences energy flow in Battery Electric Vehicles (BEV)

This chapter examines how the energy flow in the BEV changes for different drive cycles and different levels of driving aggressiveness. Because of the way the driving aggressiveness was modelled in chapter 2, the effects of velocity and acceleration can be studied separately. As described in section 2.1, three standard drive cycles, representing city, rural and highway driving were analysed using the performance parameters defined in section 4.3: energy consumption, overall average efficiency, recuperated energy, wheel work and inertia work. To allow for comparison between driving cycles, all the output parameters were distance normalized.

5.1 Effects of drive cycles on energy consumption.

First, the unmodified standard drive cycles were analysed to develop an understanding of how they influence the energy consumption in the BEV in city, rural and highway driving. Figure 5.1 illustrates how energy consumption varies with the average velocity of a driving cycle. The results are analysed separately for city, highway and rural driving.

City Cycles
The city cycles are characterized by low velocities as well as high RPA and idling values. In particular the NYCC and ArtemisURBAN cycles both have a RPA value of 0.32 m/s^2 and the highest wheel work requirement. Furthermore, they also have the lowest energy consumption due to the high amount of recuperated energy from regenerative braking (Figure 5.3) and their high average overall efficiency (Figure 5.5). The WLTClow drive cycle with the RPA of 0.22 m/s^2 is a less aggressive city cycle and requires significantly less wheel work, resulting in the lowest energy consumption of all cycles despite its correspondingly less recuperated energy and average overall efficiency.

Highway Cycles
The HWFET drive cycle on the other hand, has high average velocity and no starts

and stops, the RPA 0.07 m/s^2 and hence very little possibility for regenerative braking. It also has the lowest average overall efficiency of all drive cycles. As a result, HWFET consumes about as much energy as city or rural cycles, despite its considerably lower wheel work demand.
The US06 drive cycle has the same average velocity as HWFET, but with the RPA 0.21 m/s^2 it is a more aggressive highway cycle than HWFET. US06 can recuperate significantly more energy, but it also has higher energy consumption compared to HWFET due to its higher wheel work demand. ArtemisHW130 has the highest average velocity of these three highway cycles and with the RPA 0.14 m/s^2 is a less aggressive cycle than US06. Therefore it requires less wheel work than US06, but due to its lower average overall efficiency and recuperated energy has the highest energy consumption of all cycles.

Rural Cycles
LA92 belongs to more aggressive rural drive cycles and therefore requires more wheel work than the other rural drive cycles like ArthemisRURAL and WLTChigh. However, due to its higher energy recuperation and average overall efficiency, it has similar energy consumption as these two cycles.

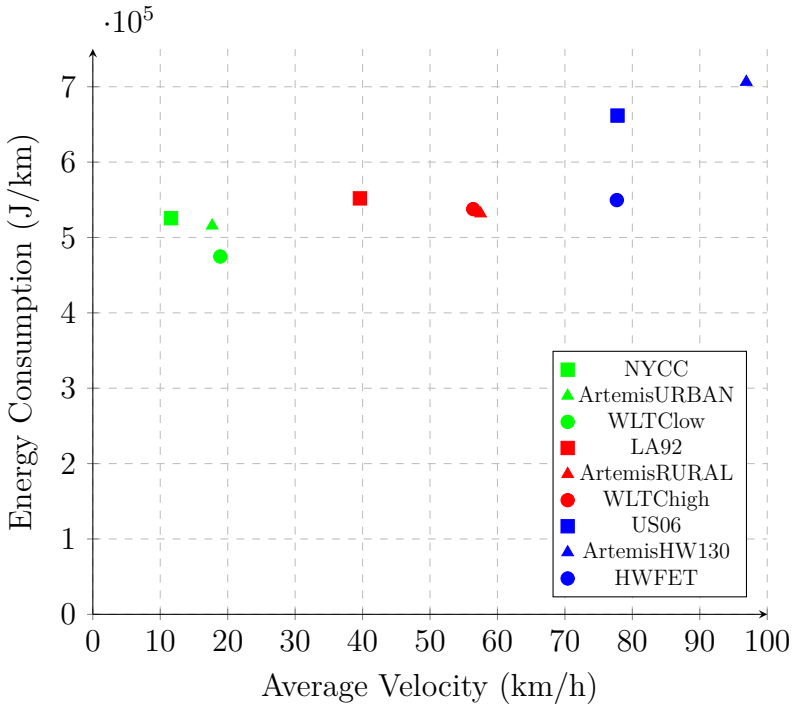

Figure 5.1: Energy consumption versus average velocity for unmodified standard drive cycles

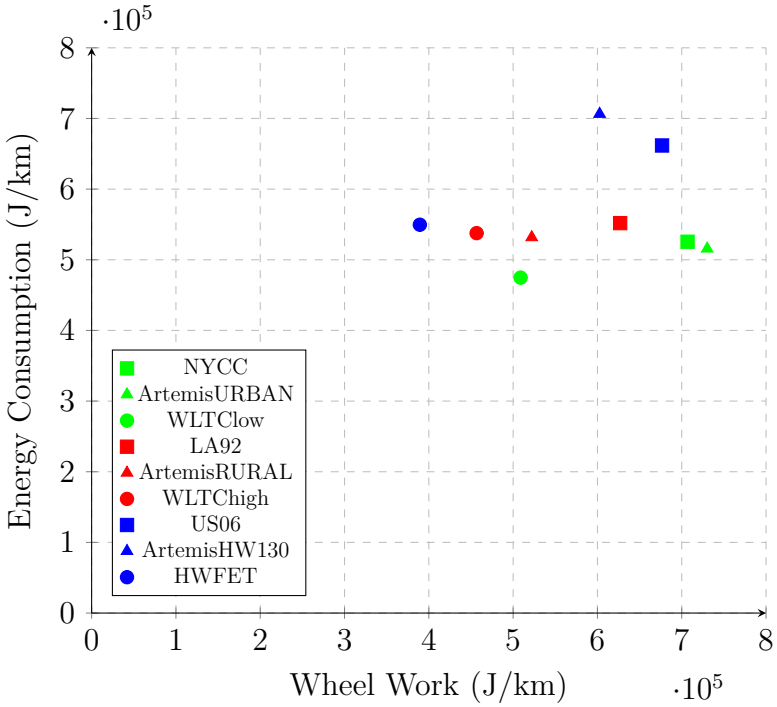

Figure 5.2: Energy consumption versus wheel work for unmodified standard drive cycles

Specific trends in the BEV energy flow (energy consumption and energy recuperation) can be observed based on the drive cycle characteristics. For that purpose, the recuperated energy versus relative positive acceleration (Figure 5.3), wheel work versus inertia work (Figure 5.4) and overall average efficiency versus average velocity (Figure 5.5) are illustrated for the selected standard drive cycles.

Average Velocity and RPA

Both higher average velocity and RPA lead to higher wheel work. US06 and WLTClow have the same RPA values, but US06 has four times higher average velocity and 33 % higher wheel work compared to WLTClow, whereas US06 has three times the RPA of HWFET at the same average velocity and requires 74 % more wheel work compared to HWFET.

Share of inertia work

Figure 5.2 shows that two city cycles NYCC and ArtemisURBAN have one of the lowest energy consumption levels despite having the highest wheel work demand. The same trend can be observed for two highway cycles US06 and ArtemisHW130, with ArtemisHW130 consuming more energy than US06 despite requiring less wheel work than US06. This result is due to energy recovered from regenerative braking. In absolute terms, recuperated energy versus RPA increases linearly as it can be seen in Figure 5.3. However, the amount of recovered energy should be discussed in relation to the required energy. In other words, drive cycles with a higher share of the inertia work, as shown in Figure 5.4, can recuperate more energy through regenerative braking. For instance, WLTClow has approximately the same wheel

work demand and energy recuperated as US06, but as a city cycle has a higher share of the inertia work than US06. In contrast, highway drive cycles with a low share of inertia work, such as HWFET or ArtemisHW130 can only recover a small fraction of their invested energy, since a large share of their wheel work requirement consists of the road work.

Both, recuperated energy and average overall efficiency reduce the energy consumption of a drive cycle. Regenerative braking, however, has a greater influence than efficiency in city cycles.

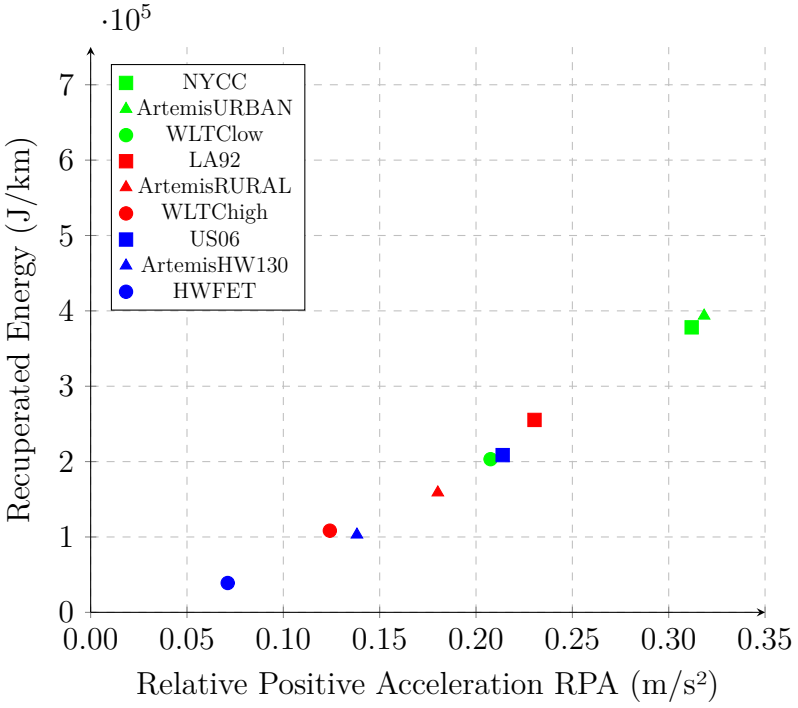

Figure 5.3: Recuperated energy versus relative positive acceleration RPA for unmodified standard drive cycles

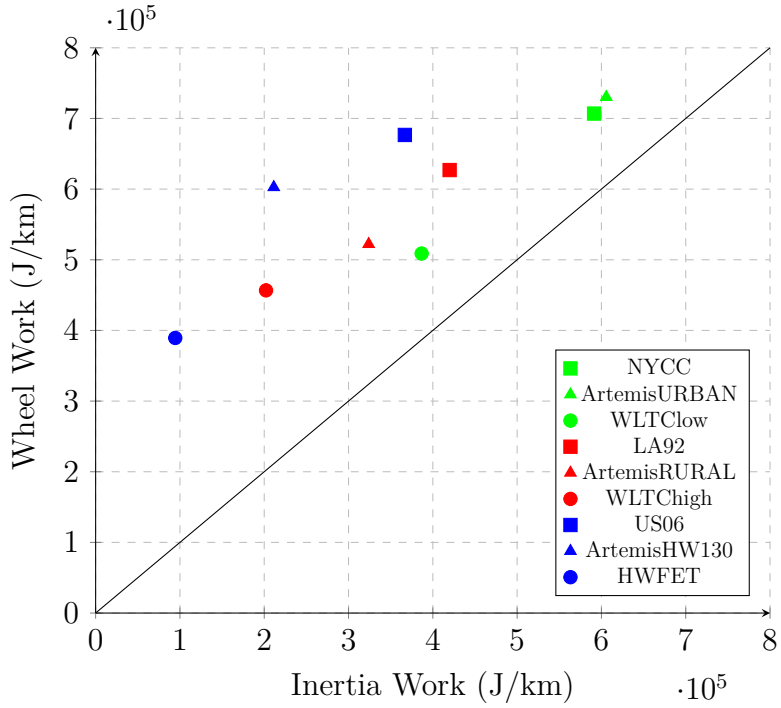

Figure 5.4: Wheel work versus inertia work for unmodified standard drive cycles

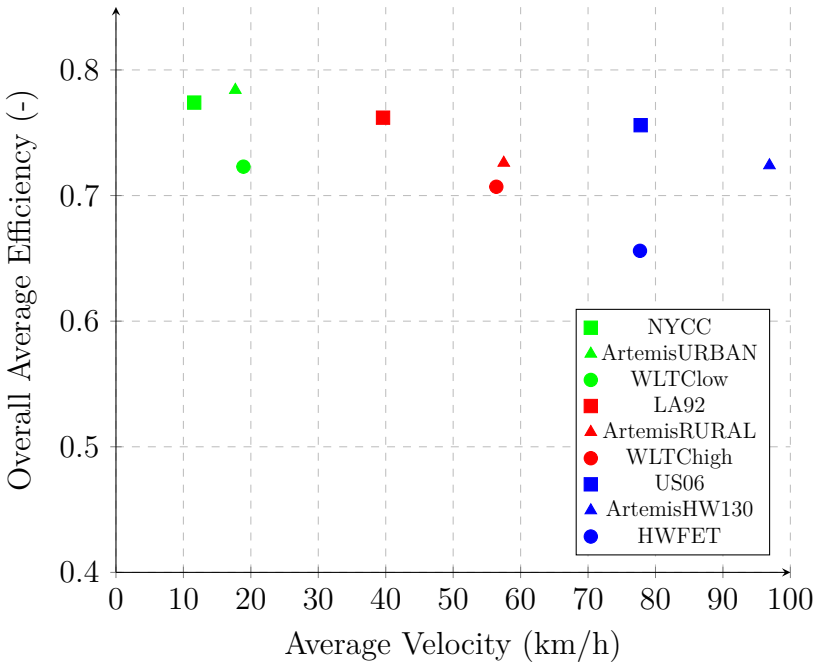

Figure 5.5: Overall average efficiency versus average velocity for unmodified standard drive cycles

5.2 Effect of velocity on energy consumption

Figure 5.6 shows how energy consumption varies with the average velocity, for velocity modified city, rural and highway drive cycles.

All cycles have the same U-shaped behavior, where energy consumption first decreases for very low velocities before increasing again. It can hence be observed that the lowest energy consumption for all cycles is between 20-30 km/h average velocity. It should be noted that a similar u-shaped behavior was found for conventional vehicles in [2], where the same explanations for this behavior apply to BEV by examining how the overall average efficiency Figure 5.8 and wheel work Figure 5.7 change with average velocity.
At low average velocity (up to 15 km/h) the average overall efficiency increases significantly with the average velocity (see Fig. 5.8) and so does the energy from regenerative braking (see Fig. 5.9), while wheel work is almost constant (see Fig. 5.7) resulting in a decrease in energy consumption. At high average velocities (>20 km/h), the average overall efficiency is almost constant, but wheel work continues to increase exponentially and the regenerative braking energy decreases, leading to a strong increase in energy consumption.

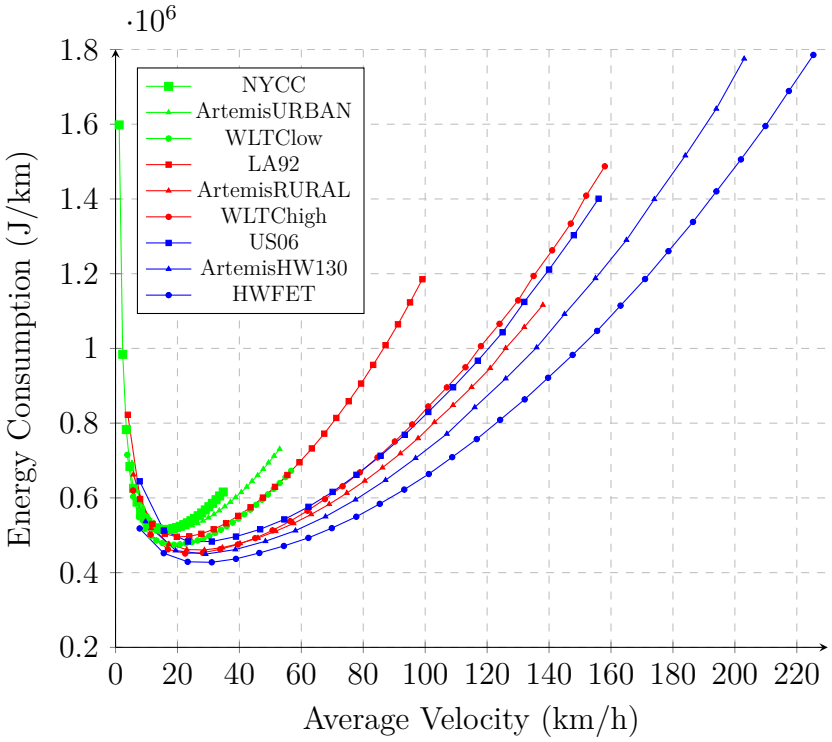

Figure 5.6: Energy consumption versus average velocity for velocity modified standard drive cycles

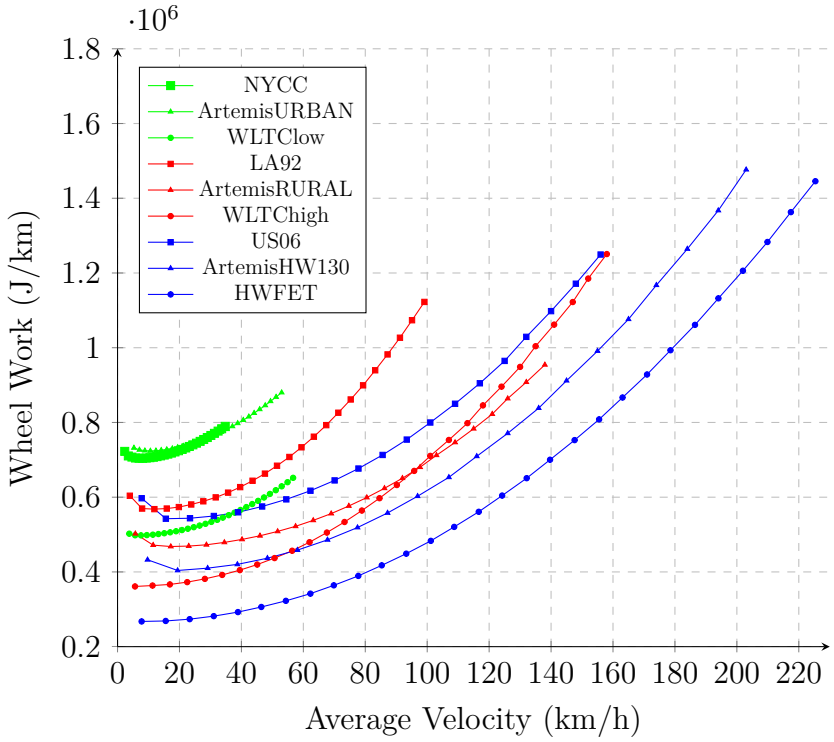

Figure 5.7: Wheel work versus average velocity for velocity modified drive cycles

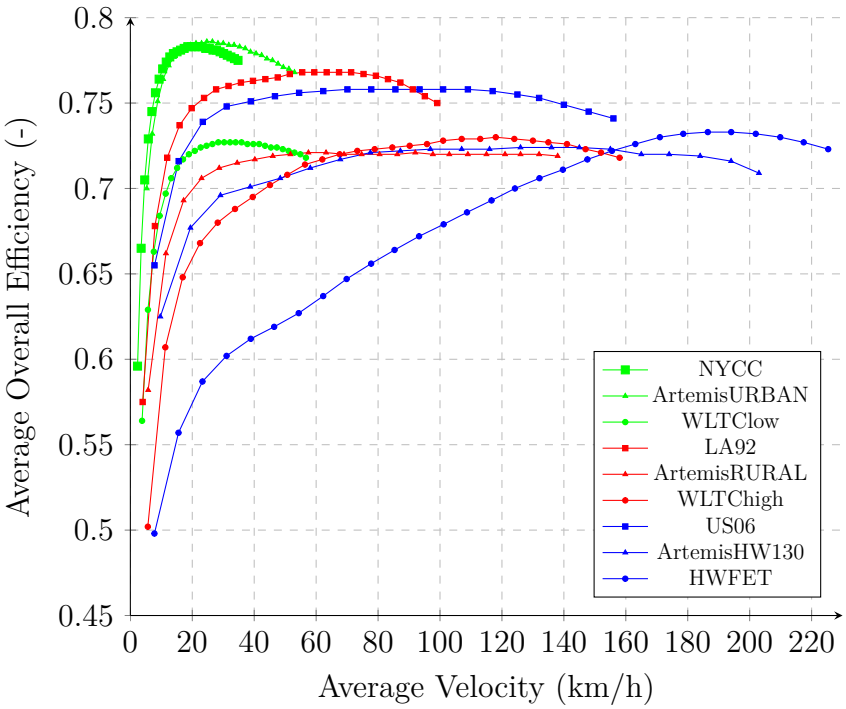

Figure 5.8: Total efficiency versus average velocity for velocity modified drive cycles

When analysing further the trend for energy recuperated from regenerative braking in Figure 5.9, a mirrored U-shaped curve is observed for all cycles except US06 and ArtemisHW130, indicating that driving at higher velocities with constant acceleration leads to less energy being recuperated during the drive cycle. Overall, city cycles like NYCC and ArtemisURBAN recuperate more energy back into the battery, but the amount of recuperated energy decreases more steeply as the average velocities increase above 15 km/h compared to rural or highway cycles.

As explained in the previous section, city cycles can recover more of their invested energy than rural or highway cycles due to higher share of inertia work. This effect is greater at low average velocities and decreases with increasing average velocities if the acceleration is kept constant. While wheel work increases exponentially, inertia work decreases with increasing average velocity (see Fig. 5.10) due to longer driving distances. Thus, the amount of energy that can be recovered from regenerative braking decreases with more aggressive driving.

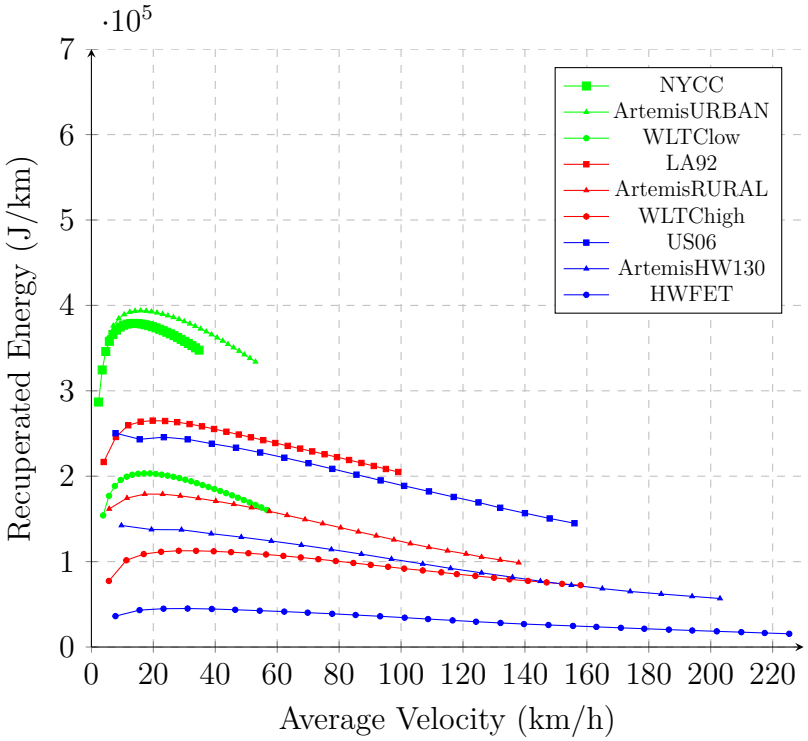

Figure 5.9: Recuperative energy versus average velocity for velocity modified drive cycles

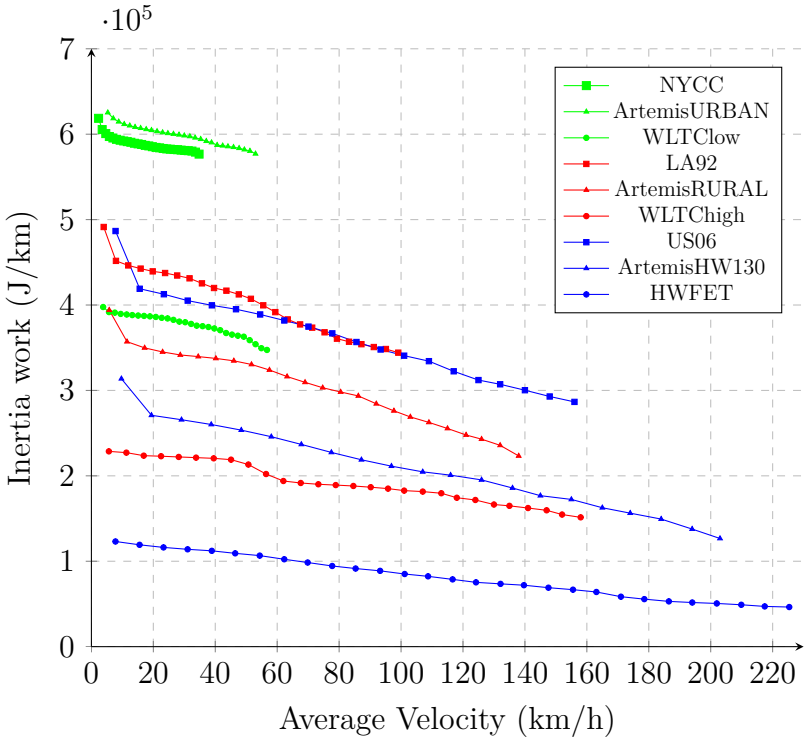

Figure 5.10: Inertia work versus average velocity for velocity modified drive cycles

5.3 Effects of acceleration on energy consumption

After having the previous section focused on the velocity modified standard drive cycles, this section analyses the behavior of the acceleration modified standard drive cycles. All drive cycles show a positively curved growth in energy consumption with increased average positive acceleration, shown in Figure 5.11. The slightly positive bending can be explained by looking at wheel work and efficiency. As it can be expected from equation 3.5, wheel work, shown in Figure 5.12, changes proportionally to acceleration if velocity is kept constant and no road gradients must be overcome. Average overall efficiency in Figure 5.13, however, rises sharply for low accelerations and flattens out at higher acceleration value, resulting in a slight upward bend in the energy consumption curve.
For trips with low average acceleration, the highway drive cycles US06 and ArtemisHW130 with high average velocities also show the highest energy consumption, followed by rural and city drive cycles. As driving becomes more aggressive, the energy consumption of highway and rural drive cycles increases at about the same rate, while that of the city cycles increase significantly sharper. The sharper growth in energy consumption for city cycles compared to highway and rural cycles is due to their high share of inertia work. Since average acceleration increases at constant velocity, only the inertia part of wheel work increases while road work remains constant. As a result, wheel work increases sharper for city cycles than for the other cycles. Figure 5.12 shows wheel work and Figure 5.14 inertia work versus average positive acceleration, respectively.

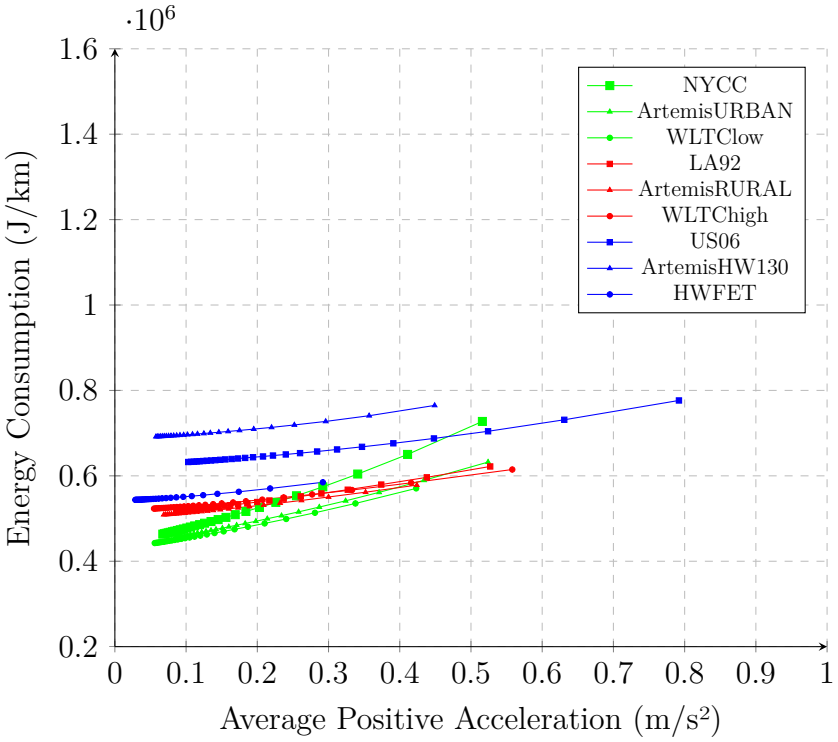

Figure 5.11: Energy consumption versus average positive acceleration for acceleration modified drive cycles

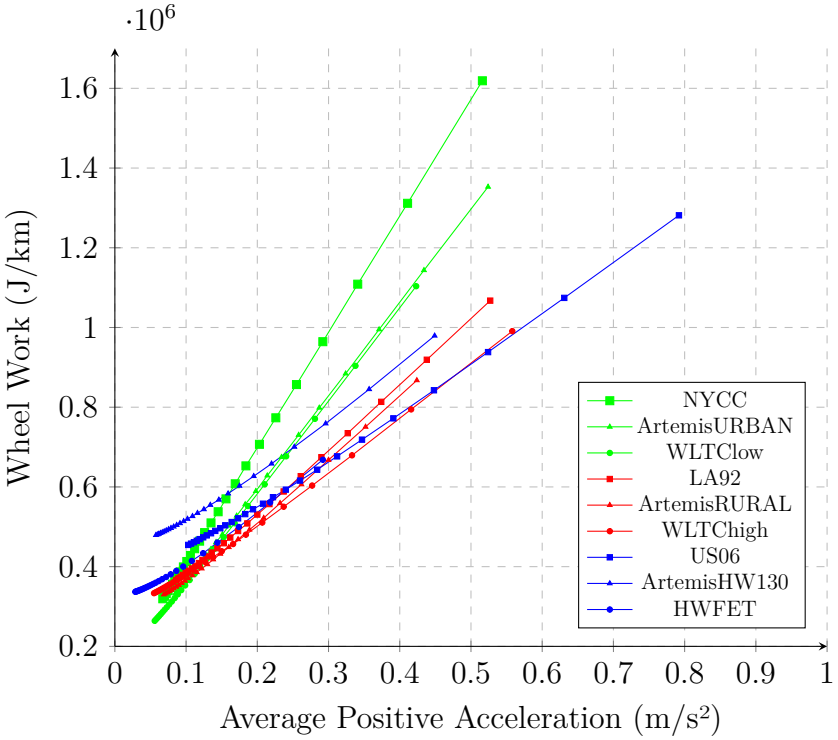

Figure 5.12: Wheel work versus average positive acceleration for acceleration modified drive cycles

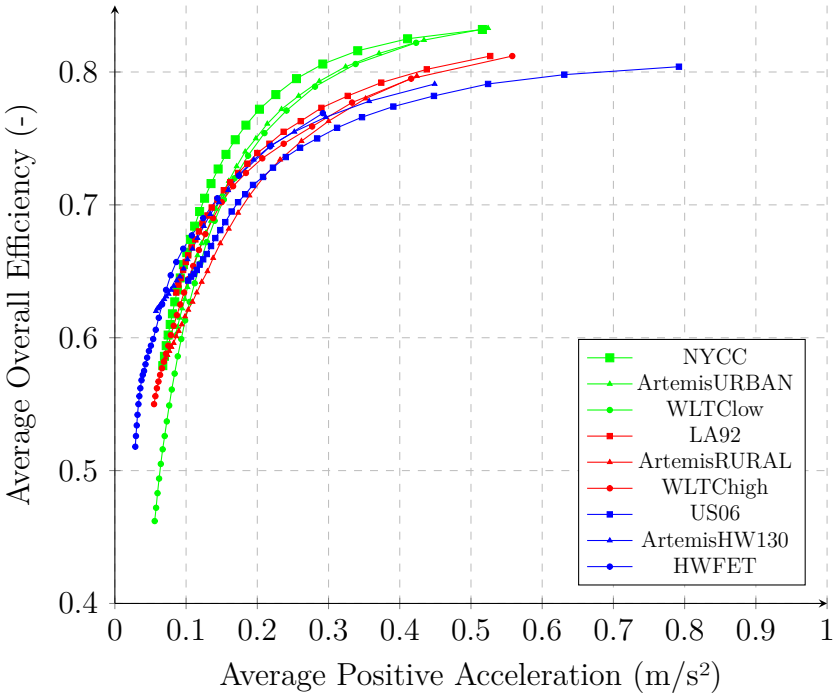

Figure 5.13: Average overall efficiency versus average positive acceleration for acceleration modified drive cycles

The increase in the inertia work correlates with the increase in recuperated energy, shown in Figure 5.15. This means that the more aggressive the driving behavior is, the more energy is required, but can also be recovered through regenerative braking. City cycles in particular have the highest potential to recuperate energy through regenerative braking.

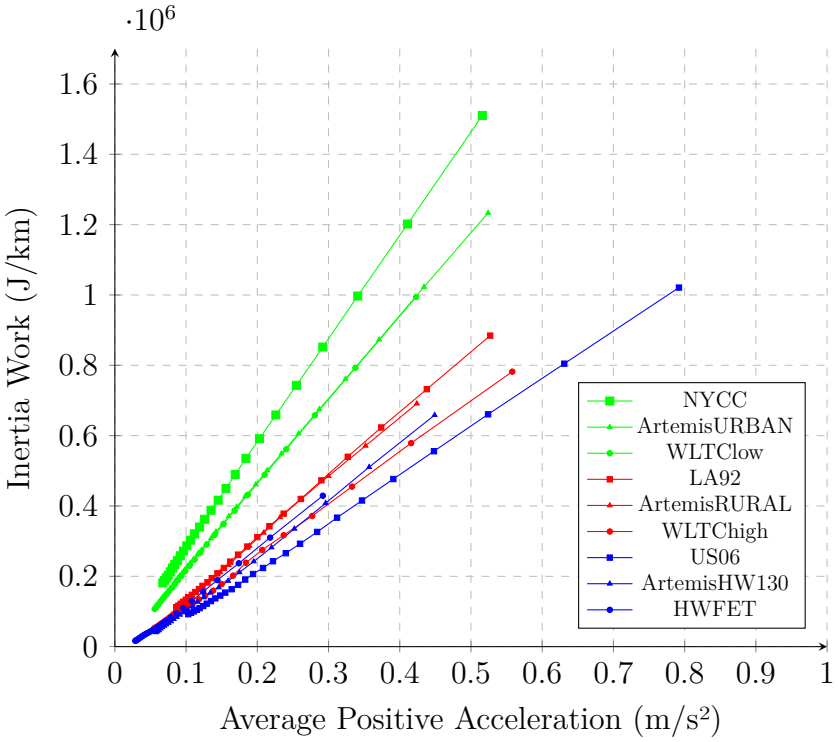

Figure 5.14: Inertia work versus average positive acceleration for acceleration modified drive cycles

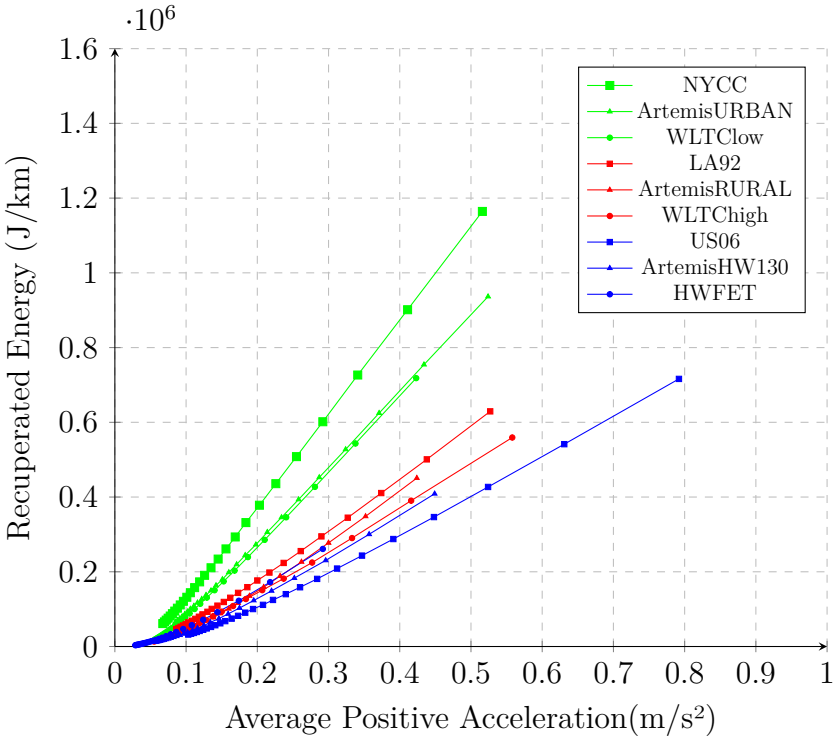

Figure 5.15: Recuperated energy versus average positive acceleration for acceleration modified drive cycles

6

Energy consumption sensitivity to driving aggressiveness

This chapter quantifies the sensitivity of energy consumption to changes in wheel work for different levels of driving aggressiveness using standard drive cycles. Sensitivity is described using the definition from [11] and shown in Equation 6.1,

$$\Gamma_{Wheel}^{Energy} = \frac{\frac{E_{Energy}}{d}}{\frac{E_{Wheel}}{d}} = \frac{E_{con}}{W_{Wheel}} \tag{6.1}$$

where Γ_{Wheel}^{Energy} is the sensitivity of energy consumption to wheel work, d is the distance travelled, E_{Energy} is the amount of energy consumed and E_{Wheel} is the energy needed at the wheels for driving. By defining sensitivity in this way, it is possible to compare different drive cycles of various lengths, since both energy consumption and wheel work are distance normalised. Therefore, sensitivity can simply be seen as the gradient of energy consumption as a function of wheel work, which can easily be displayed graphically.

The sensitivity was determined by placing trend lines through the points of the individual batches. The curve fitting tool in Matlab was used to generate these trend lines. Depending on the course of the batches, the trend lines were adjusted.

6.1 Sensitivity for velocity modified drive cycles

The energy consumption for city cycles shown in Figure 6.1, follows a U-shaped profile for different levels of driving aggressiveness (corresponding to wheel work changes). To construct straight lines which fit best the data, two first-order polynomials, one for each of the descending (Gradient decreasing) and the ascending (Gradient increasing) energy consumption profiles were used and shown in the corresponding color for each cycle. The same approach to the sensitivity assessment was applied to the rural cycles in Figure 6.2 and to the highway cycles in Figure 6.3.

The U-shaped behavior can be clearly observed for city cycles. The lowest energy consumption corresponds to the highest overall efficiency (Fig. 5.8) and the highest amount of energy recuperated from regenerative braking (see Fig. 5.9). For rural cycles, the U-curve occurs at very low driving aggressiveness, while the behavior is negligible for highway cycles. Looking at the values for Gradient increasing for highly aggressive driving in Table 6.1, it can be seen that the city cycles show the highest sensitivity, followed by the rural and highway cycles.
In the part of the U-curve with descending energy consumption that corresponds to low levels of driving aggressiveness, wheel work is nearly constant or even increased. The values for Gradient decreasing show much greater sensitivity of energy consumption to wheel work for less aggressive driving.

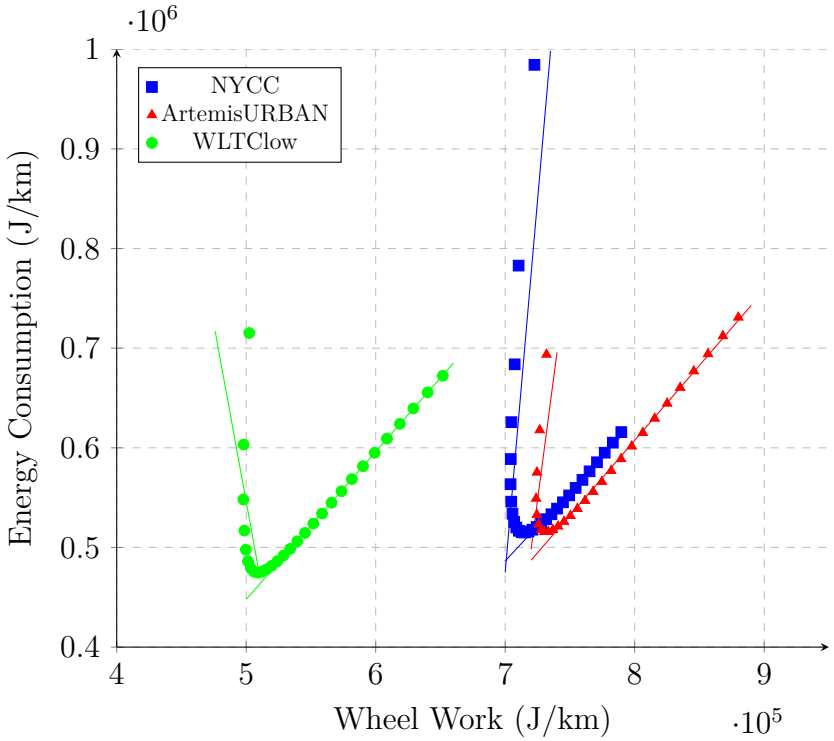

Figure 6.1: Energy consumption versus wheel work for velocity modified city drive cycles with trend lines

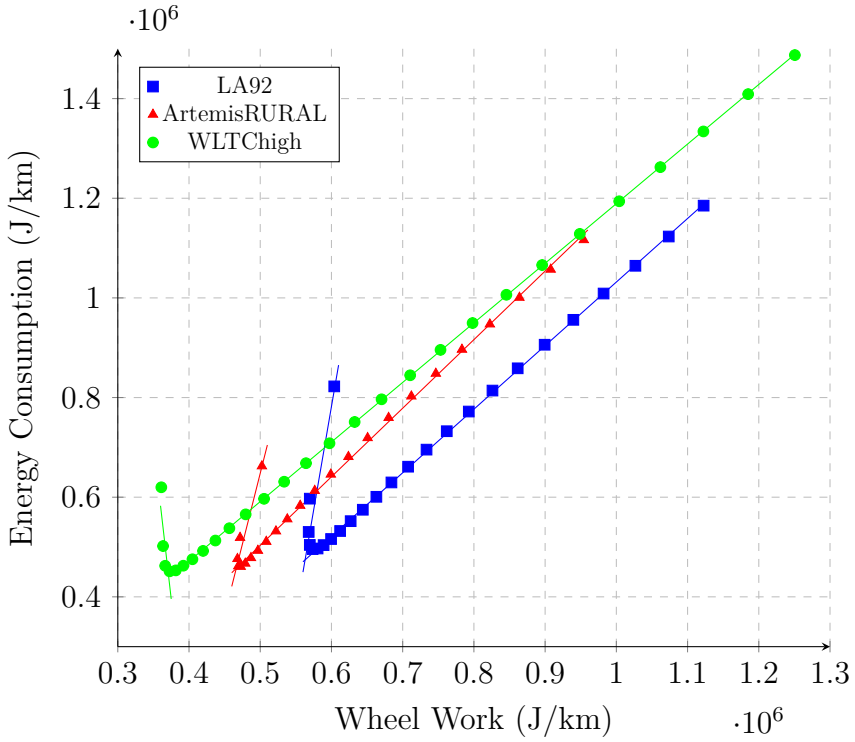

Figure 6.2: Energy consumption versus wheel work for velocity modified rural drive cycles with trend lines

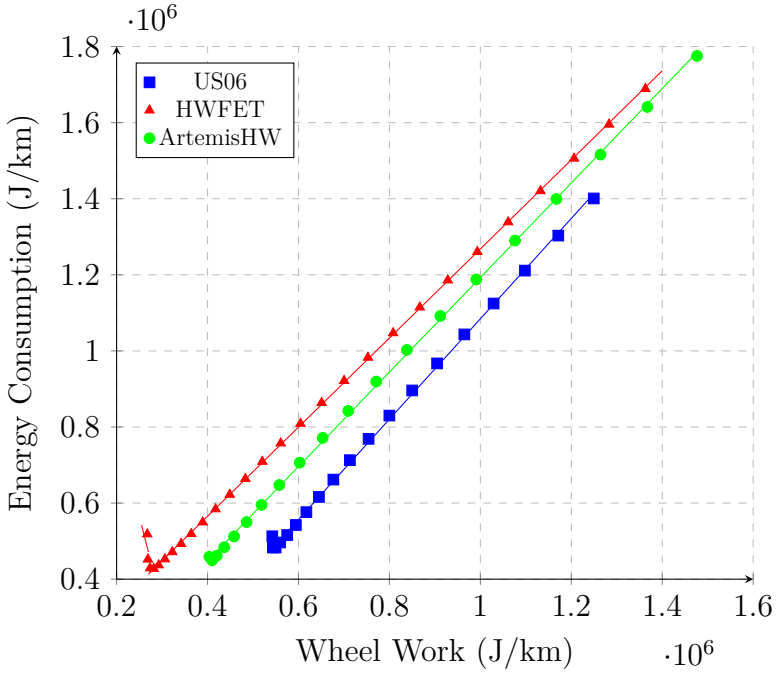

Figure 6.3: Energy consumption versus wheel work for velocity modified highway drive cycles with trend lines

Table 6.1: Sensitivity analysis for velocity modified standard drive cycles

	Gradient decreasing	Gradient increasing
NYCC	14.95	1.40
ArtemisURBAN	9.87	1.50
WLTClow	-7.13	1.49
LA92	8.31	1.28
ArtemisRURAL	5.58	1.38
WLTChigh	-12.47	1.20
US06	n.a	1.32
HWFET	-4.76	1.17
ArtemisHW130	n.a	1.24

6.2 Sensitivity for acceleration modified drive cycles

The sensitivity for acceleration modified drive cycles was captured with two first-order polynomials to fit the slightly increased sensitivity that occurs at higher accelerations.

At constant velocity, it can be seen that energy consumption rises nearly linear with increasing wheel work. Simulation results for city cycles are shown in Figure 6.4, for rural cycles in Figure 6.5 and for highway cycles in Figure 6.6. As presented in Table 6.2, city cycles have the highest sensitivity to changes in wheel work, highway cycles have the second highest and rural cycles the lowest values. Compared to velocity modified driving it is noticeable that acceleration modified driving is significantly less sensitive to changes in wheel work.

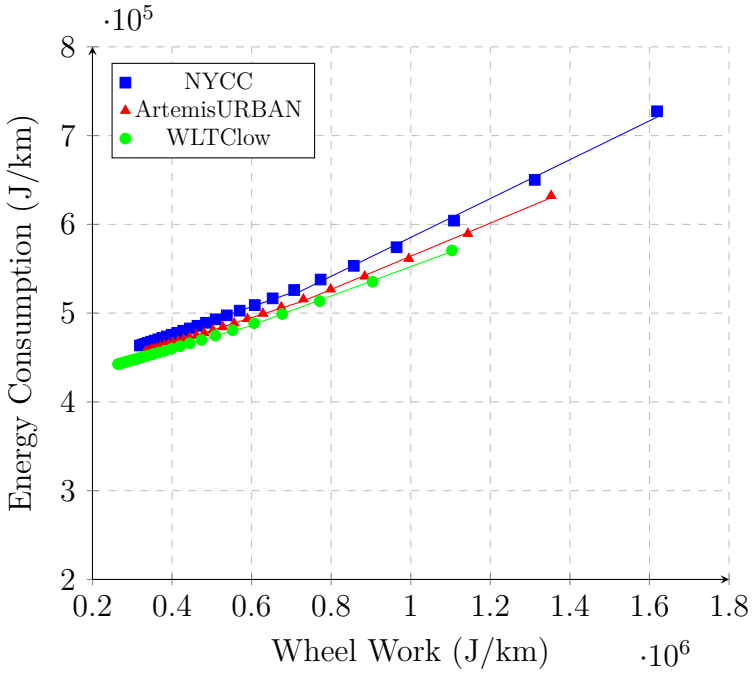

Figure 6.4: Energy consumption versus wheel work for acceleration modified city drive cycles

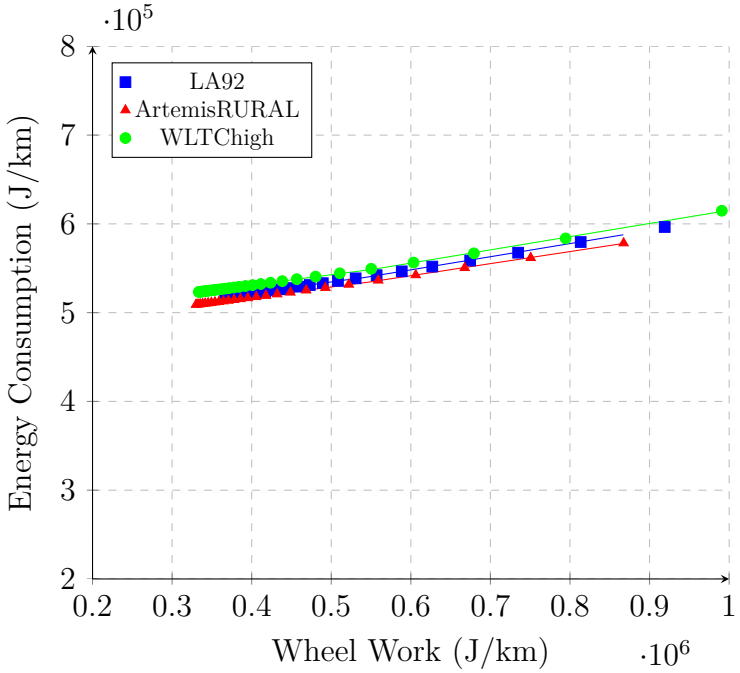

Figure 6.5: Energy consumption versus wheel work for acceleration modified rural drive cycles

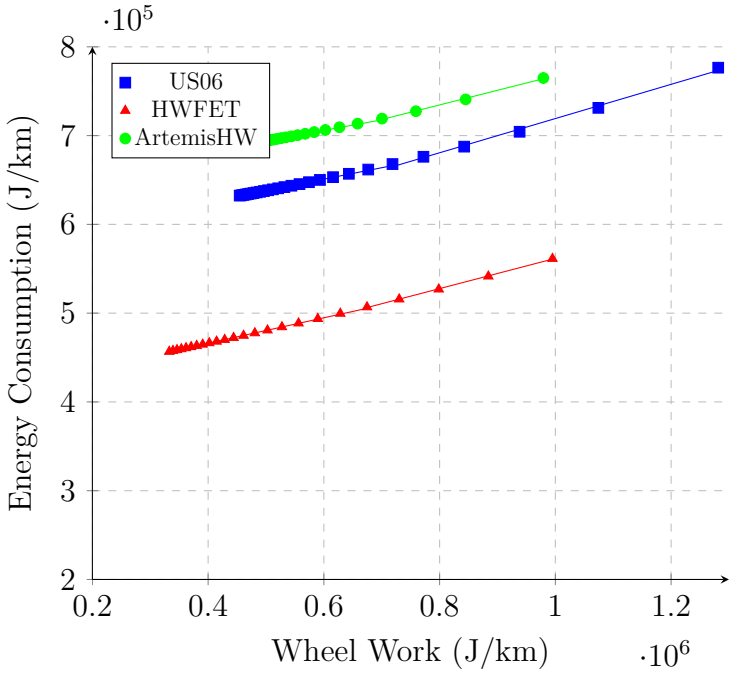

Figure 6.6: Energy consumption versus wheel work for acceleration modified highway drive cycles

Table 6.2: Sensitivity analysis for acceleration modified standard drive cycles

	Gradient low	Gradient high
NYCC	0.16	0.22
ArtemisURBAN	0.14	0.19
WLTClow	0.13	0.17
LA92	0.13	0.15
ArtemisRURAL	0.12	0.14
WLTChigh	0.12	0.15
US06	0.13	0.19
HWFET	0.14	1.17
ArtemisHW130	0.12	0.16

7

Logged real-world drive patterns

In this chapter, the previous results of the standard drive cycles are compared with real-world drive patterns. For this purpose, data from an earlier study [7] were used and the real-world drive cycles were modified according to the methodology described in Section 2.2. Since the real-world drive patterns are also characterized by a distance-dependent vehicle altitude profile in addition to the time-dependent velocity profile, the BEV-model was extended by signal components presented in Figure 4.6, adjusting the vehicle elevation profile accordingly. The labels high-speed, middle-speed and low-speed correspond to highway, rural and city driving, respectively.

7.1 Comparison between logged real-world drive patterns

First, the influence of different unmodified real-world drive patterns on energy consumption is analysed. Due to the large number of real-world patterns, these are plotted in corresponding groups. City cycles are shown in green, rural cycles in red and highway cycles in blue.
As expected from the way the drive patterns are categorized, the high-speed patterns have the highest average velocities, followed by the middle- and low-speed patterns, as presented in Figure 7.1. In contrast, Figure 7.2 shows that the high-speed patterns have lower average positive accelerations compared to the middle- and low-speed patterns. The energy consumption is higher for high-speed than for middle-speed patterns, while the low-speed patterns display a variety in energy consumption from the lowest middle-speed consumption levels to the consumption higher than in the high-speed patterns. Looking at wheel work versus energy consumption in Figure 7.3, shows that high-speed patterns consume a relatively large amount of energy compared to their low wheel work demand. Most of the middle- and low-speed patterns require more wheel work than the high-speed patterns, but have lower energy consumption. The reason is the same as for the standard drive cycles. The low- and middle-speed patterns have a higher share of inertia work and can therefore recuperate more of the invested energy, as it can be seen in Figure 7.4.

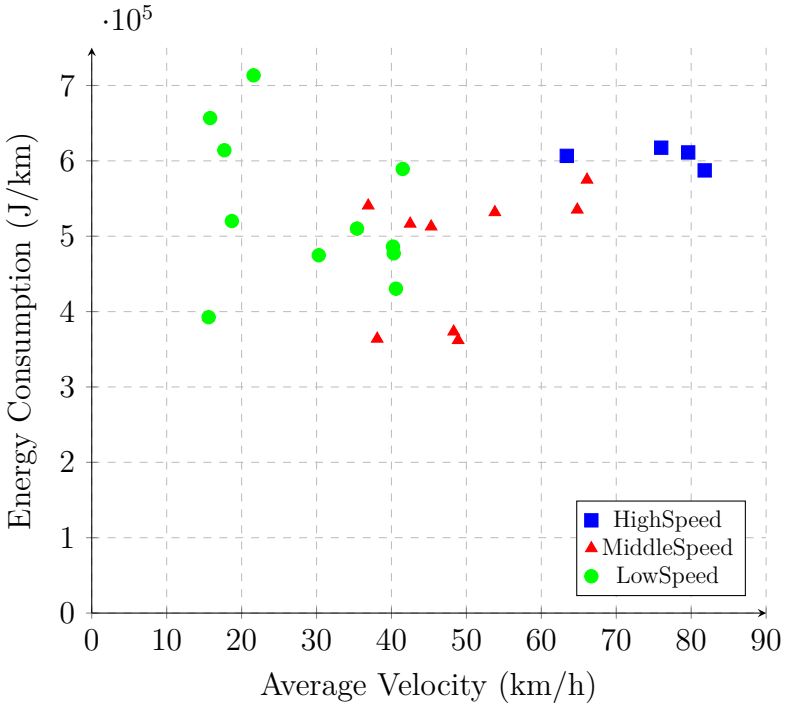

Figure 7.1: Energy consumption versus average velocity for logged real-world drive patterns

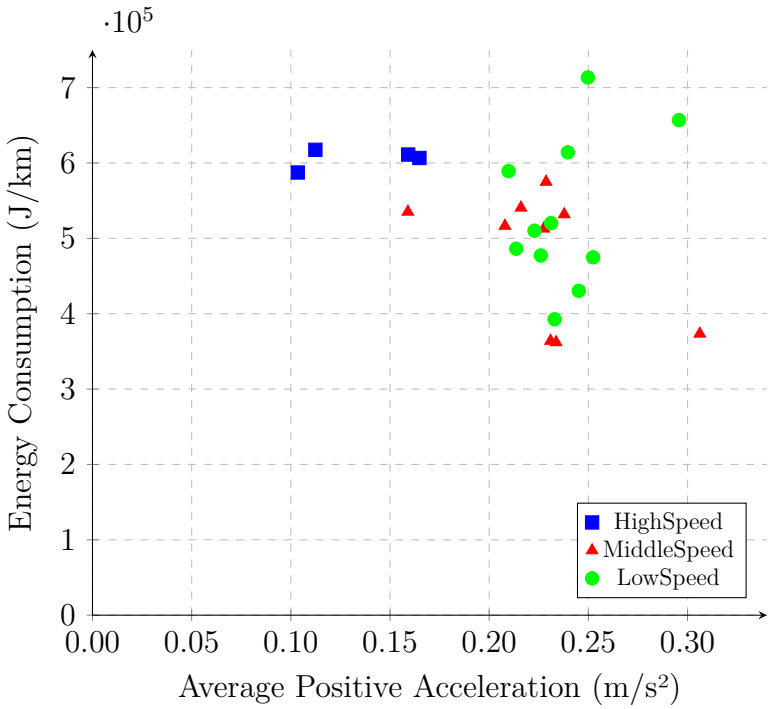

Figure 7.2: Energy consumption versus average positive acceleration for real-world logged drive patterns

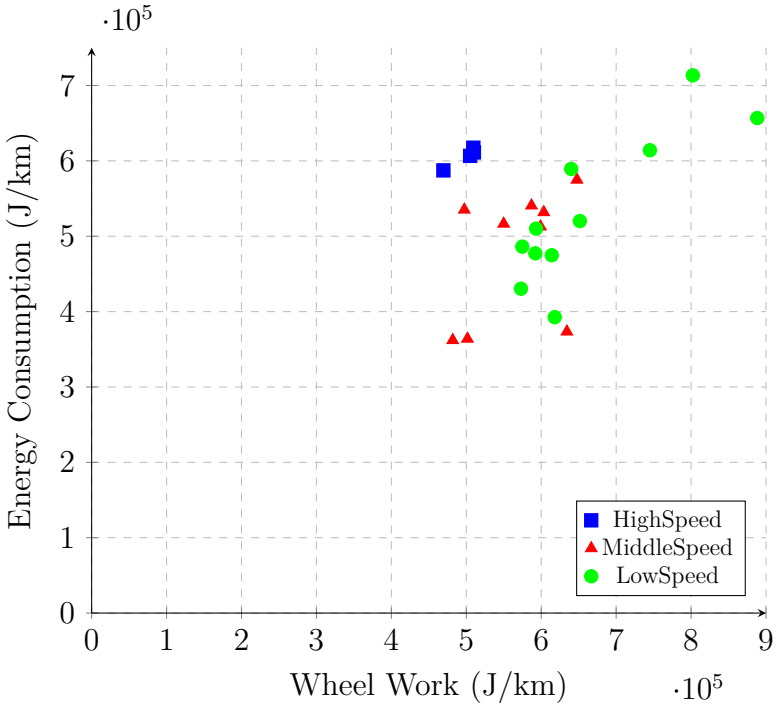

Figure 7.3: Energy consumption versus wheel work for real-world logged drive patterns

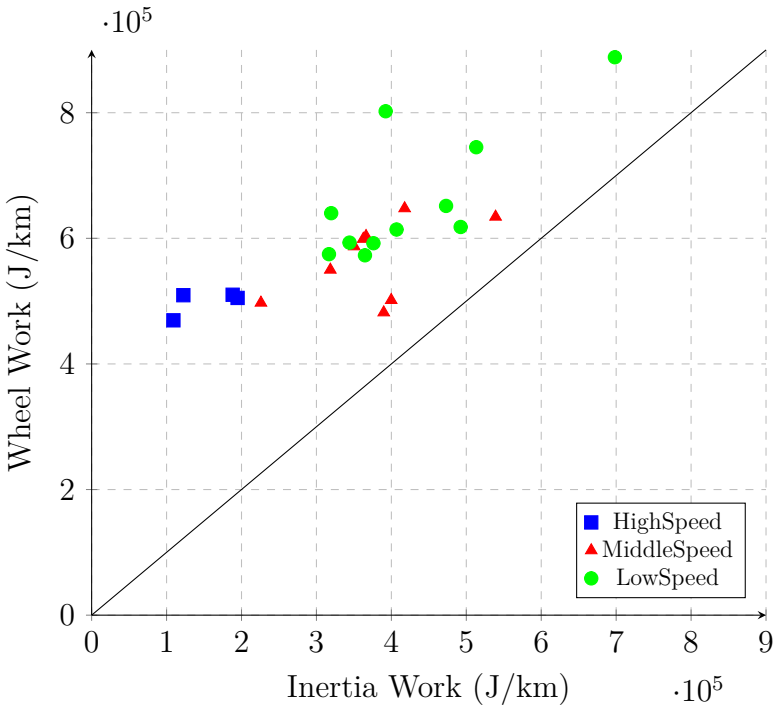

Figure 7.4: Wheel work versus inertia work for real-world logged drive patterns

For the logged patterns, a similar proportional increase in the recuperated energy versus RPA as for standard drive cycles can be seen in Figure 7.5

Figure 7.6 shows energy consumption versus the vehicles altitude difference between the start and the end of the logged drive patterns. The negative values indicate more downhill and the positive ones more uphill driving. For the middle- and low-speed patterns, it can be seen that downhill driving reduces energy consumption, while uphill driving increases energy consumption. This trend cannot be observed as clearly for the high-speed patterns.

The average overall efficiency, displayed in Figure 7.7, shows that the low-speed drive patterns that represent city driving are the most efficient drive patterns followed by the middle- and high-speed drive patterns.

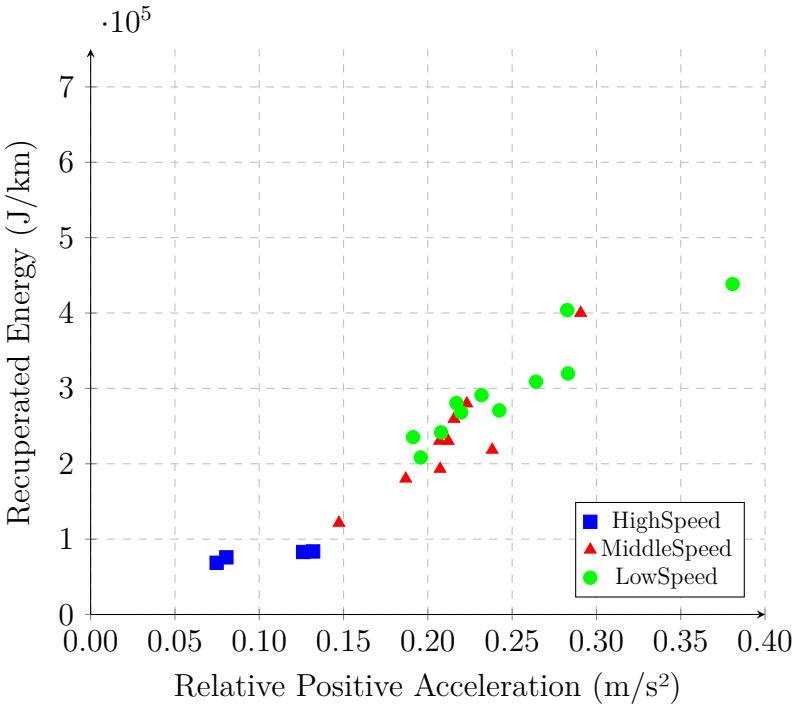

Figure 7.5: Recuperated energy versus RPA for real-world logged drive patterns

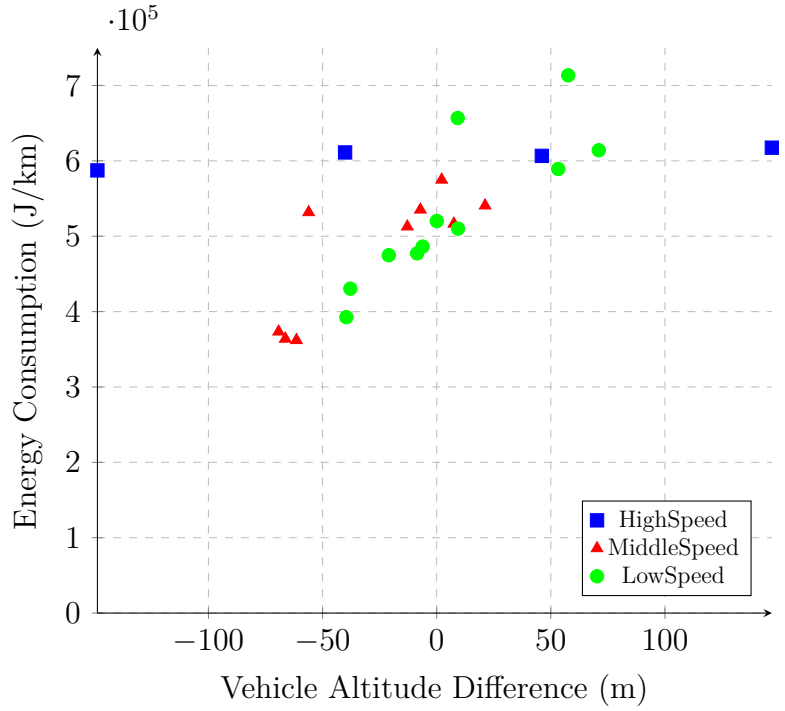

Figure 7.6: Energy consumption versus vehicle altitude difference for real-world logged drive patterns

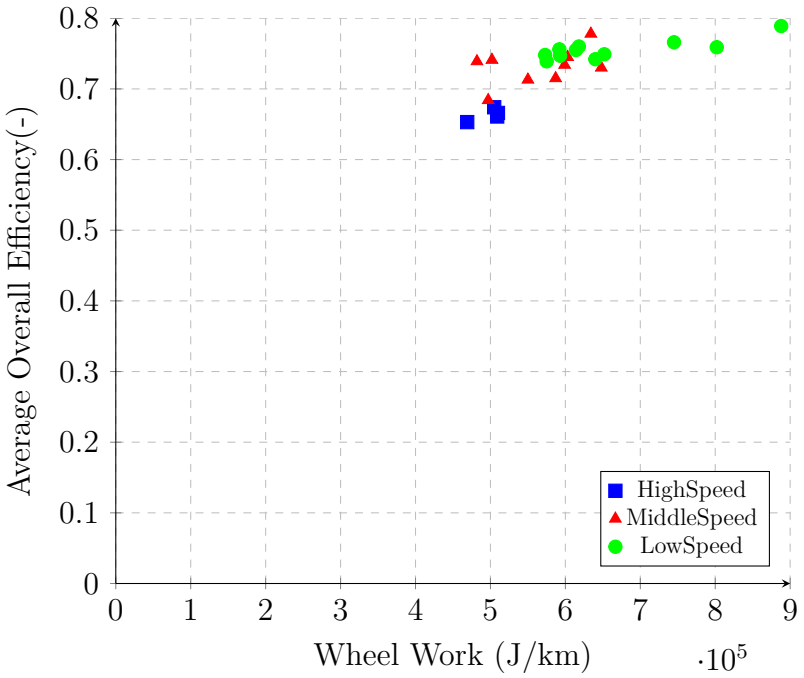

Figure 7.7: Total efficiency versus wheel work for real-world logged drive patterns

add figure

7.2 Comparison between standard and real-world driving for velocity modified drive patterns

The following sections compare the behavior of the standard drive cycles and logged drive patterns. For this purpose one logged and one standard cycle each in the categories city, rural and highway are taken and velocity modified. In the following sections, city cycles (NYCC, LS9) are plotted in blue, rural cycles (ArtemisRURAL, MS2 AtoB) in red and highway cycles (HWFET; HS1 AtoB) in black.

Observing the energy consumption over average velocity in Figure 7.8, the logged drive patterns show the same u-shaped behavior as the standard drive cycles. The lowest energy consumption for the logged cycles is similar to standard drive cycles (between 20-40 km/h).

In the average velocity range 10-40 km/h, LS9 has lower energy consumption than the high-speed patterns despite its higher wheel work. Aside from more recuperated energy, as discussed for standard drive cycles, this could be due to the road slope that real-world drive patterns possess. In contrast to NYCC, LS9 is a downhill drive pattern with a height difference of -40 m, thus it can also use energy recovered by the negative road slope for regenerative driving. Due to this, LS9 can recuperate more energy than NYCC, although LS9 has less inertia work, as shown in Figure 7.12. HS1 AtoB on the other hand is an uphill drive pattern with an altitude difference of 50 m and MS2 AtoB a slightly downhill drive pattern with an altitude difference of -10 m. Both behave similar to their standard drive cycle counterparts without any noticeable influence of the road slope.

When comparing the standard drive cycles with the real-world logged patterns, the influence of the road slope on wheel work must not be overlooked. The road slope is already included in the calculation of wheel work. However, since wheel work by definition considers the integral of tractive power only when tractive power is positive, wheel work does not reflect the influence of the road slope during downhill driving completely.
An alternative way for further studies to determine the energy required to complete a drive cycle would be wheel energy.

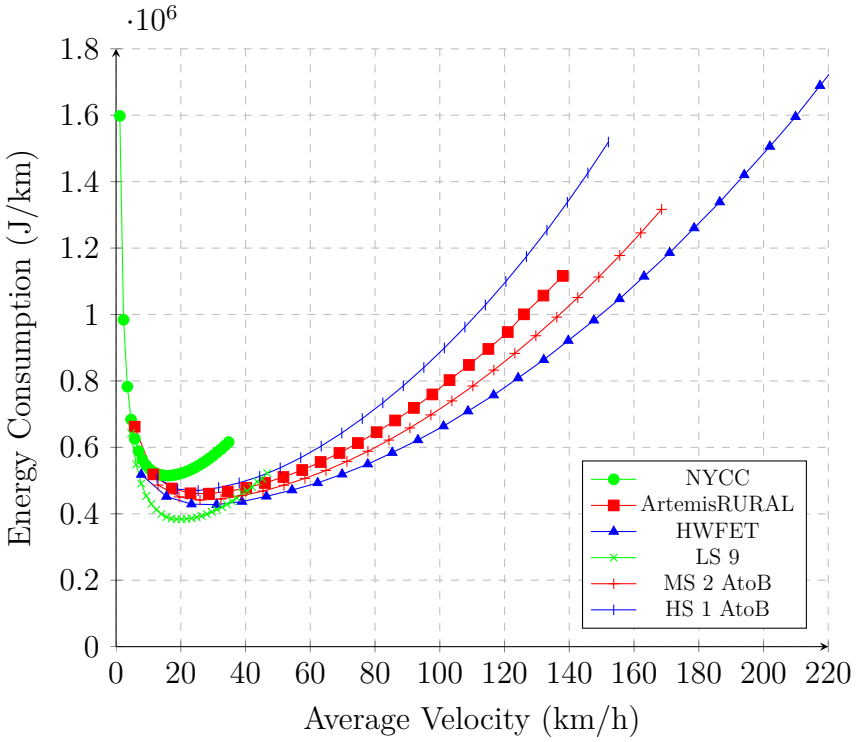

Figure 7.8: Energy consumption versus average velocity for velocity modified standard and real-world drive cycles

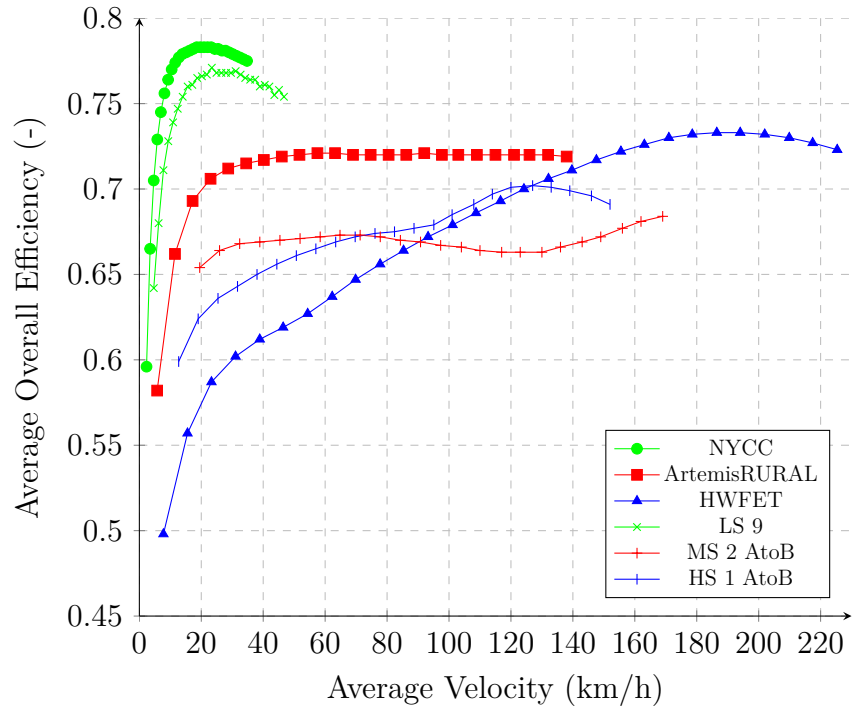

Figure 7.9: Average overall efficiency versus average velocity for velocity modified standard and real-world drive cycles

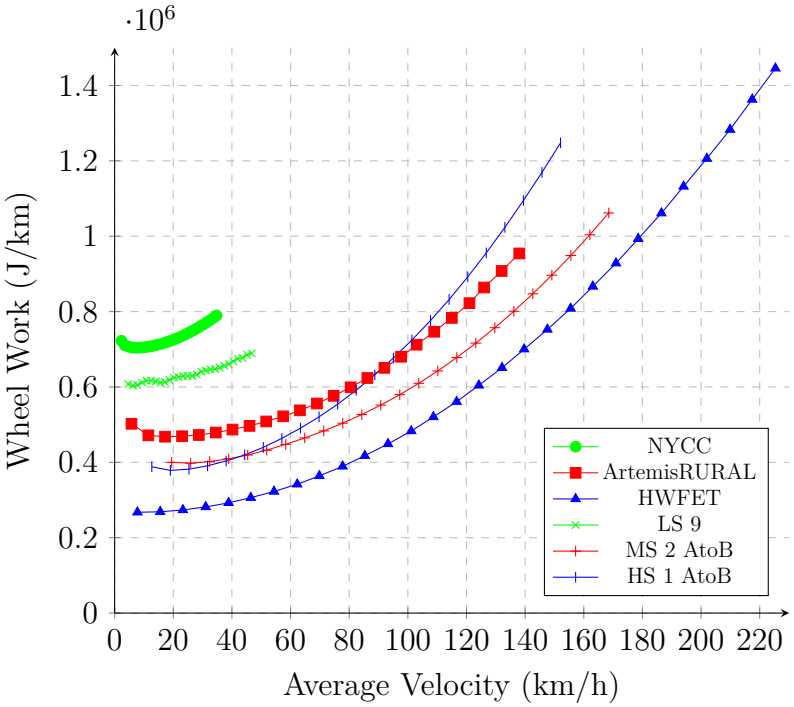

Figure 7.10: Wheel work versus average velocity for velocity modified standard and real-world drive cycles

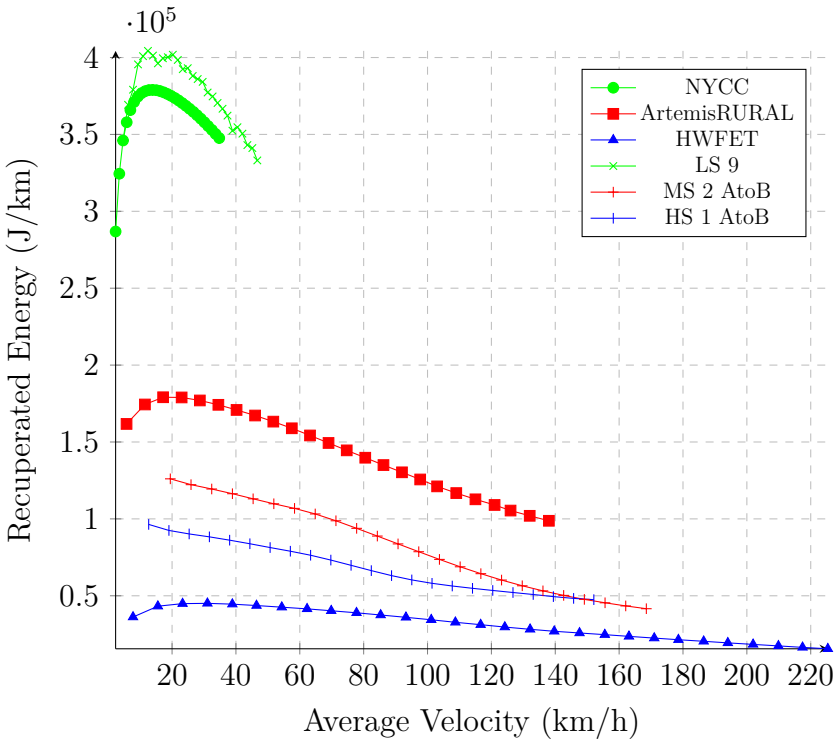

Figure 7.11: Recuperated energy versus average velocity for velocity modified standard and real-world drive cycles

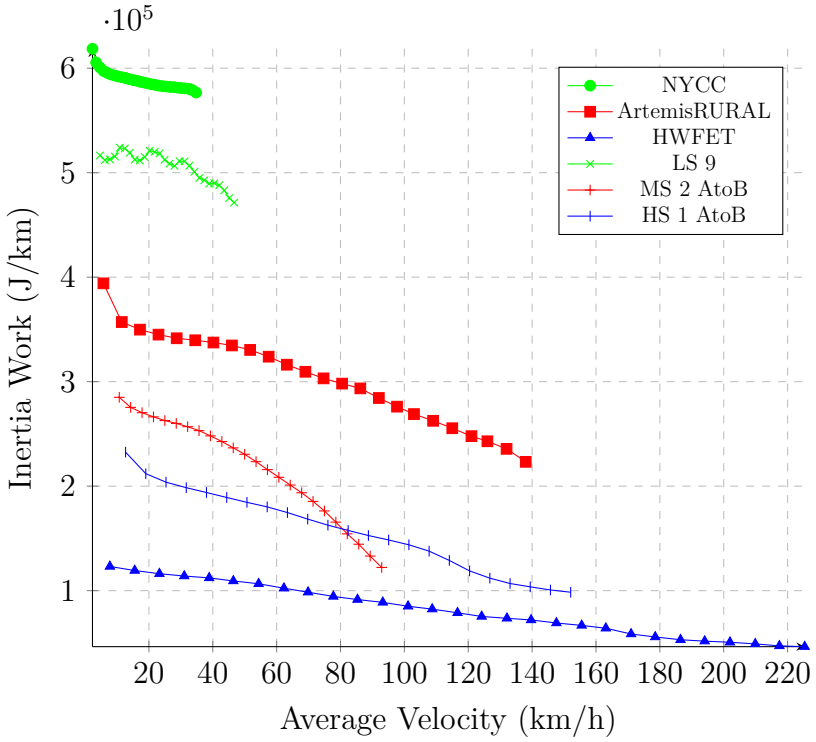

Figure 7.12: Inertia work versus average velocity for velocity modified standard and real-world drive cycles

7.3 Comparison between standard and real-world driving for acceleration modified drive patterns

After comparing velocity modified cycles in the previous section, acceleration modified standard drive cycles and real-world drive patterns will be discussed.

The depiction of energy consumption over the average acceleration for logged drive patterns in Figure 7.13 is consistent with the results for the corresponding standard drive cycles presented in Section 5.3. When driving at low accelerations, high-speed patterns show the highest energy consumption, followed by the middle- and low-speed patterns. LS9 shows significantly lower energy consumption compared to NYCC due to downhill driving.

Wheel work in Figure 7.14 and average overall efficiency in Figure 7.15 show similar behavior for the real-world patterns as for the standard drive cycles. Looking at the inertia work versus the average positive acceleration in Figure 7.16, LS9 recovers more energy than NYCC at the average positive acceleration below 0.15 m/s^2, despite the larger inertia work in NYCC (see Fig. 7.17).

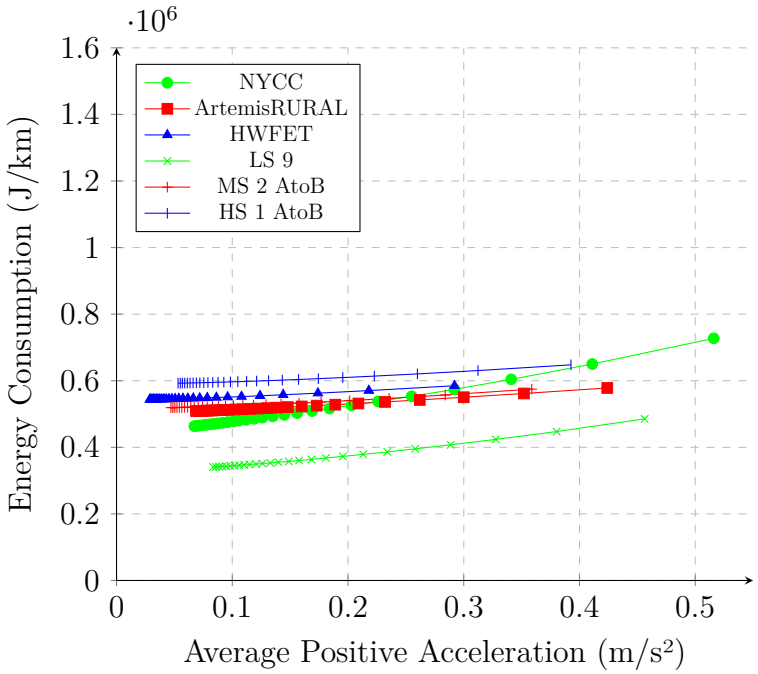

Figure 7.13: Energy consumption versus average positive acceleration for acceleration modified speed traces for standard and real-world drive cycles

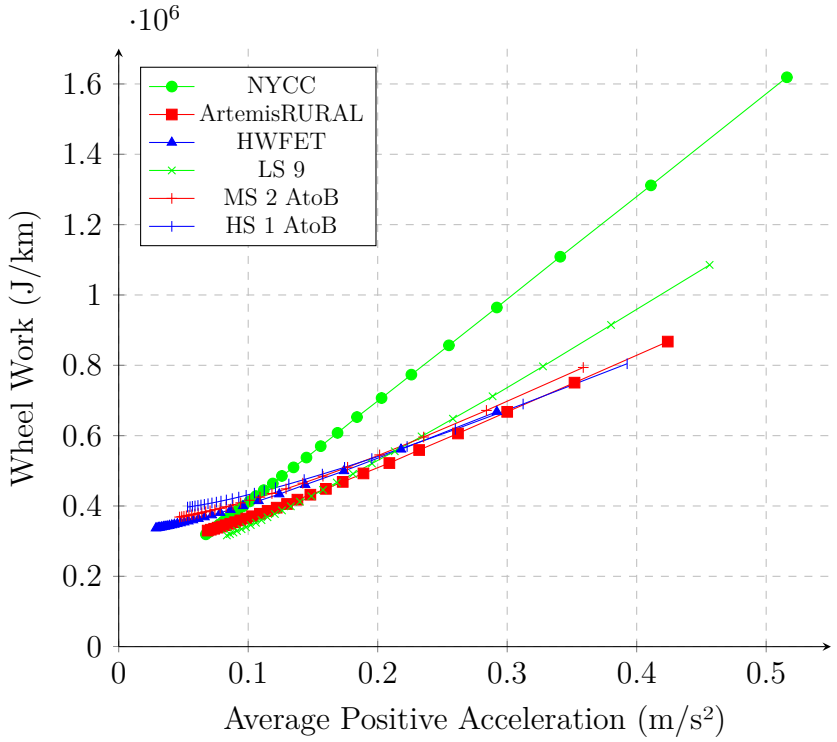

Figure 7.14: Wheel work versus average positive acceleration for acceleration modified speed traces for standard and real-world drive cycles

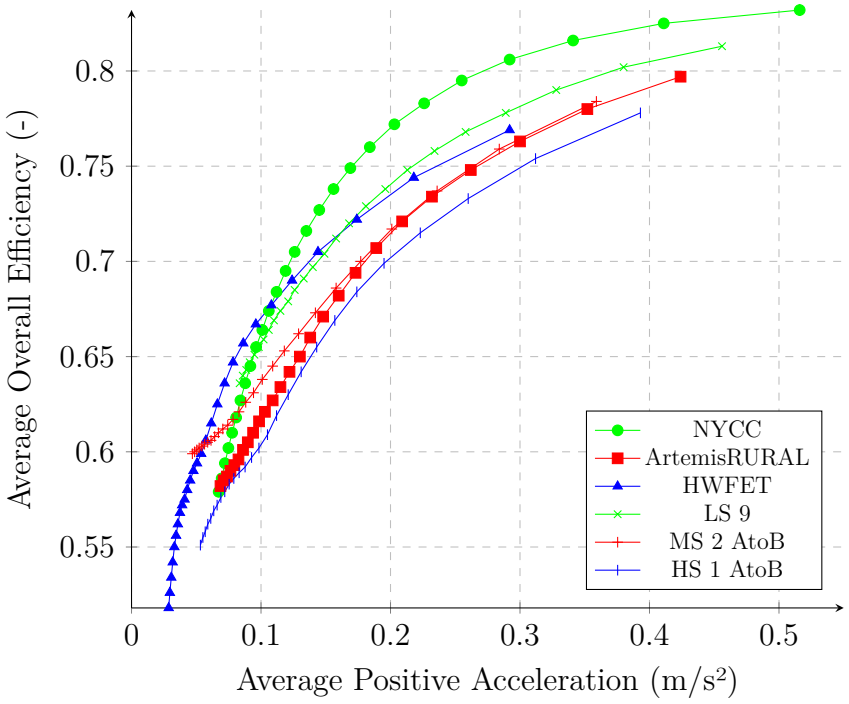

Figure 7.15: Average overall efficiency versus average positive acceleration for acceleration modified speed traces for standard and real-world drive cycles

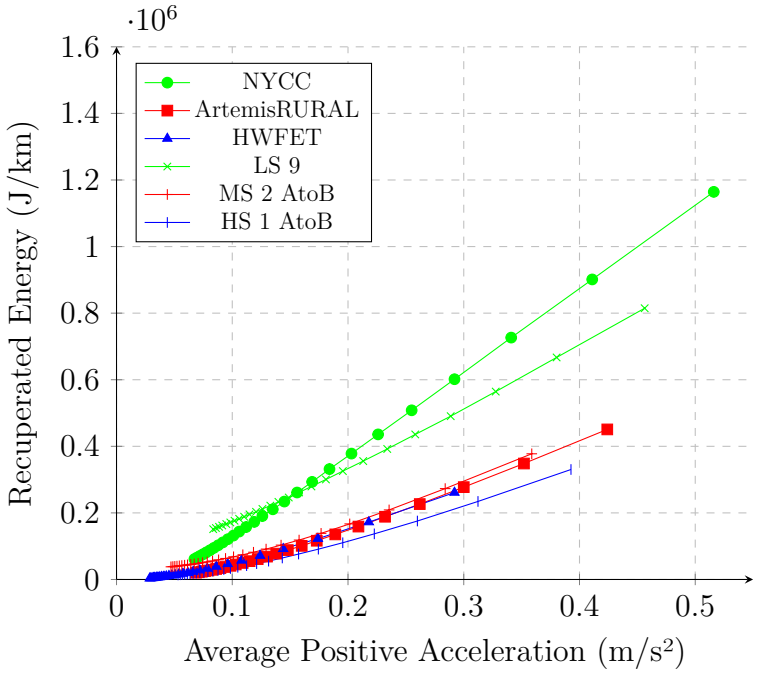

Figure 7.16: Recuperated energy versus average positive acceleration for acceleration modified speed traces for standard and real-world drive cycles

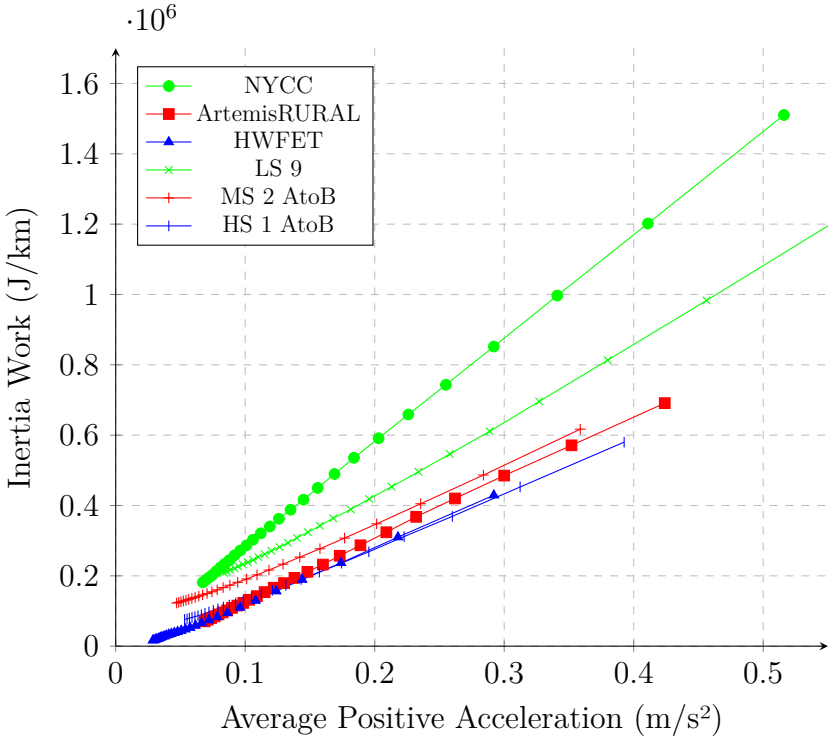

Figure 7.17: Inertia work versus average positive acceleration for acceleration modified speed traces standard and real-world drive cycles

7.4 Comparison of energy consumption sensitivity between standard drive cycles and real-world drive patterns

Part of analysing the behavior of energy consumption is to quantify the sensitivity of energy consumption towards wheel work between the standard drive cycles and the real-world patterns. Energy consumption versus wheel work is plotted for velocity modified driving in Figure 7.18, Figure 7.19 and Figure 7.20 for city, rural and highway cycles, respectively. The results for the acceleration modified patterns are plotted in Figure 7.21, Figure 7.22 and Figure 7.23 for city, rural and highway driving, respectively. Sensitivity is defined as the gradient between energy consumption and wheel work, as explained in chapter 6. The same method for creating the fitting lines of standard drive cycles has been used for real world patterns.

Table 7.1 shows the sensitivity values for the velocity modified drive patterns. Overall, the logged drive patterns show the same gradation, with city cycles being the most sensitive to changes in wheel work, followed by rural and highway cycles. Comparing the increasing gradients, the logged low-speed city cycles, especially LS 9, show higher sensitivity than standard drive cycles (see Tab. 6.1). The middle-speed rural cycles also have increased sensitivity values, whereas for the high-speed highway cycles similar sensitivity as for standard drive cycles can be observed.

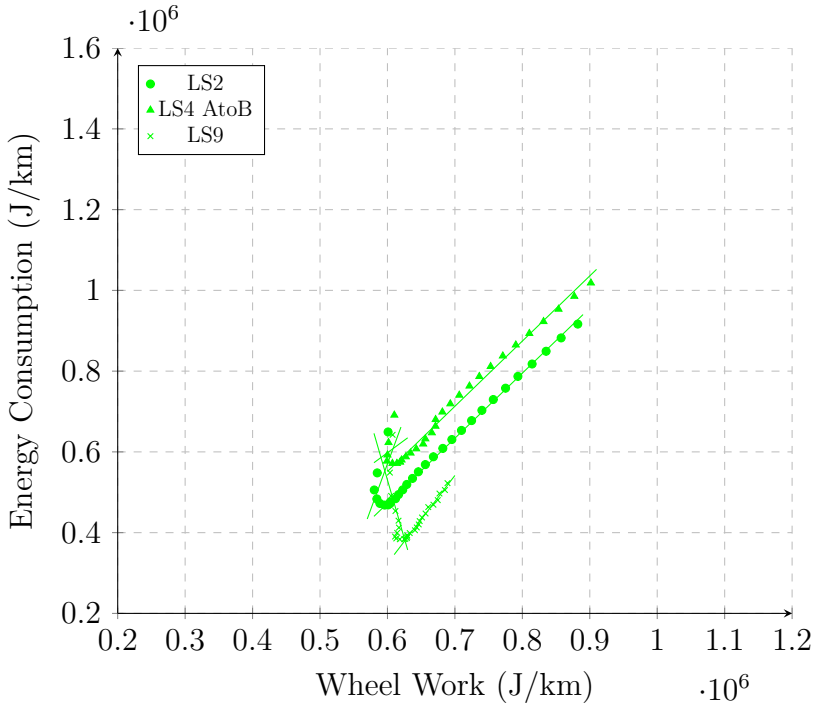

Figure 7.18: Energy consumption versus wheel work for velocity modified real-world city drive patterns

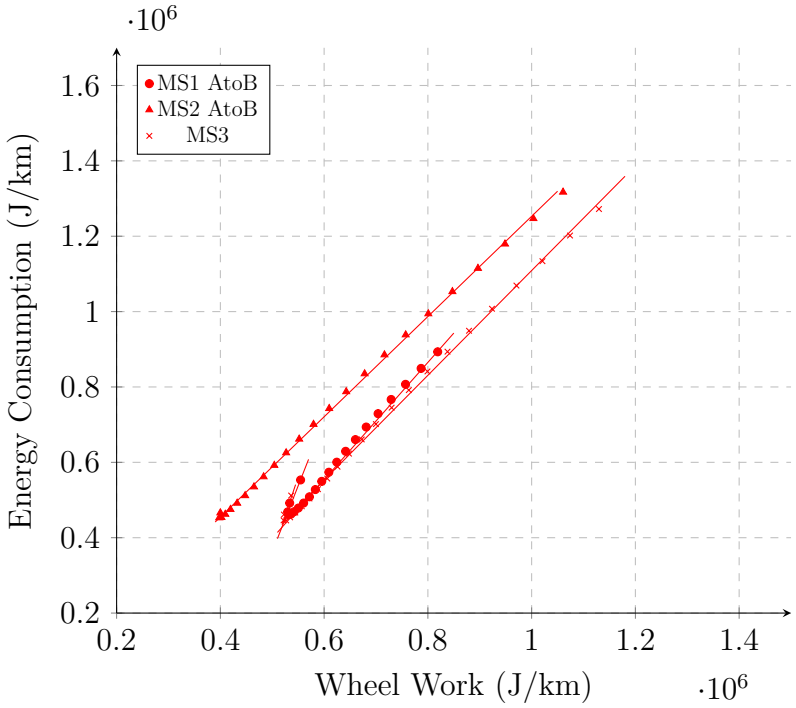

Figure 7.19: Energy consumption versus wheel work for velocity modified real-world rural drive patterns

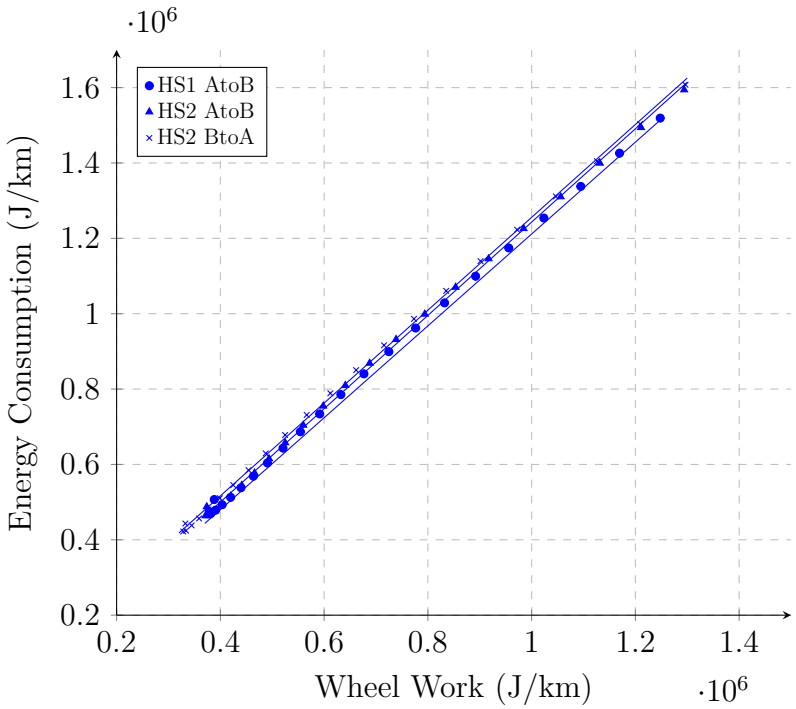

Figure 7.20: Energy consumption versus wheel work for velocity modified real-world highway drive patterns

Table 7.1: Energy consumption sensitivity for velocity modified real-world drive patterns

	Gradient decreasing	Gradient increasing
LS 2	4.55	1.61
LS 4 AtoB	-5.78	1.62
LS 9	-5.78	2.18
MS 1 AtoB	3.51	1.56
MS 2 AtoB	N.A.	1.33
MS 3	4.11	1.40
HS 1 AtoB	N.A.	1.22
HS 2 AtoB	N.A.	1.34
HS 2 BtoA	N.A.	1.23

The corresponding sensitivity values for the acceleration modified drive patterns can be found in Table 7.2. It can be seen that the logged drive patterns have slightly lower overall sensitivity values compared to the standard drive cycles in Table 6.2.

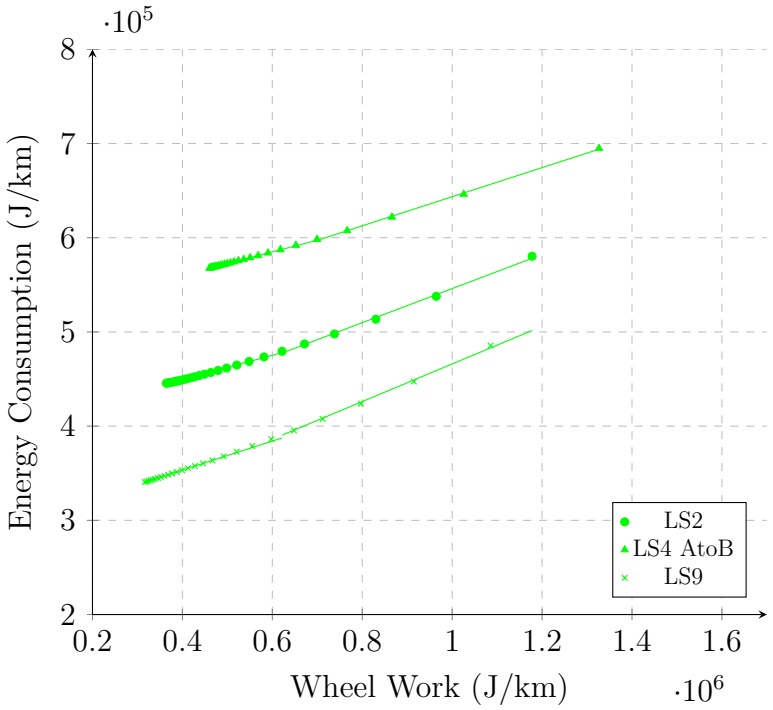

Figure 7.21: Energy consumption versus wheel work for acceleration modified real-world low-speed drive patterns

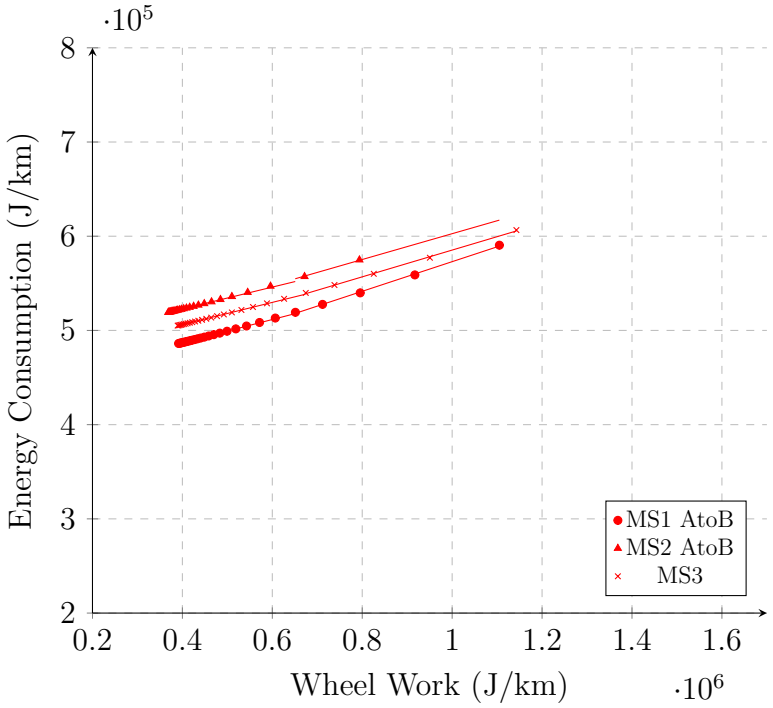

Figure 7.22: Energy consumption versus wheel work for acceleration modified and real-world middle-speed drive patterns

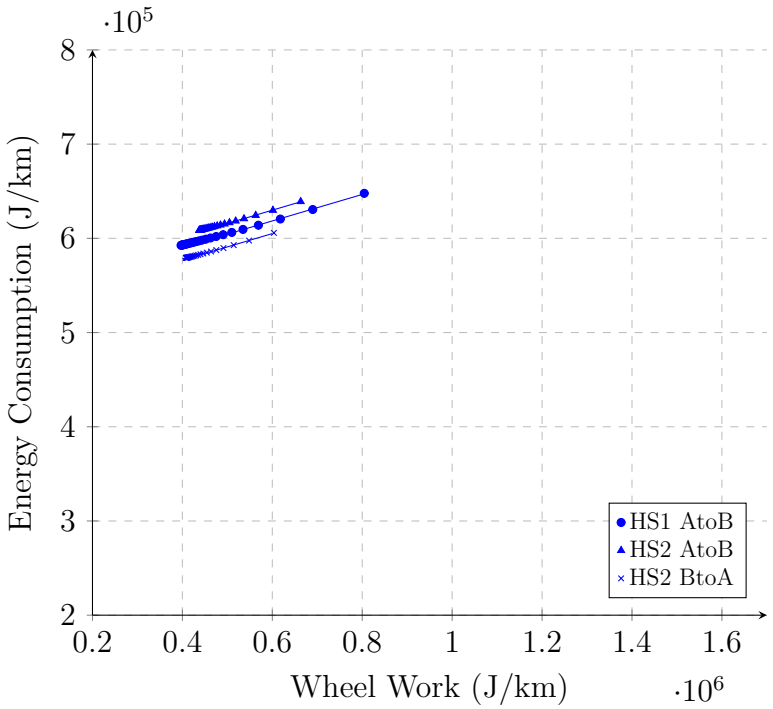

Figure 7.23: Energy consumption versus wheel work for acceleration modified and real-world high-speed drive patterns

Table 7.2: Energy consumption sensitivity for acceleration modified real-world drive patterns

	Gradient low	Gradient high
LS 2	0.13	0.18
LS 4 AtoB	0.12	0.15
LS 9	0.15	0.20
MS 1 AtoB	0.12	0.16
MS 2 AtoB	0.12	0.14
MS 3	0.12	0.14
HS 1 AtoB	0.12	0.14
HS 2 AtoB	0.12	0.14
HS 2 BtoA	0.12	0.14

8

Conclusions

Vehicle-level simulations were performed in this thesis to investigate the effects of driving aggressiveness on energy flow in the Battery Electric Vehicle (BEV). Standard drive cycles and real-world logged drive patterns [1] were considered for city, rural and highway driving.

8.1 Effects of drive cycles on energy consumption

Highway drive cycles with low Relative Positive Acceleration (RPA) values (steady-speed driving) such as HWFET require considerably less wheel work than city or rural drive cycles. However, higher wheel work demand does not automatically correspond to higher energy consumption in BEVs. Especially city and rural drive cycles with lower average velocities and high RPA values consume less energy than it would be expected based on their high wheel work. This is primarily due to the ability of BEVs to recover parts of their invested energy through regenerative braking.

Thus, BEVs are most suitable for city driving, as the low velocity and high amount of power demanding accelerations result in a high inertia work share. On the other side, high velocity drive cycles with high RPA not only require more wheel work, but a large part of their wheel work consists of road work which cannot be used for energy recuperation.

8.2 Effects of velocity modified driving behavior on energy consumption

The results presented in this thesis demonstrate the U-shape behavior for energy consumption versus the average velocity similarly to fuel consumption for conventional vehicles. Driving at very low average velocities leads to strong decrease in the average overall efficiency and therefore to sharp increase in energy consumption. Driving at high average velocities leads to higher wheel work and thus to increase in energy consumption. This U-shaped behavior is particularly evident for the city cycles, and less pronounced for the rural and highway cycles. The lowest energy consumption for all cycles is at average velocities between 20-30 km/h.

For velocity modified drive patterns where the accelerations remain constant, only

the road work part of wheel work is changed and it increases quadratically with velocity. As a result, the proportional share of the inertia work declines with velocity and so does the amount of energy recuperated through regenerative braking. This decrease in recuperated energy is the reason BEVs have higher energy sensitivity for city cycles than for rural and highway cycles.

The identified behaviors for standard drive cycles have also been observed in the logged real-world drive patterns, though the influence of road slopes requires further research.

8.3 Effects of acceleration modified driving behavior on energy consumption

For the acceleration modified drive patterns energy consumption varies linearly with wheel work. As expected, lower accelerations lead to lower energy consumption for all cycles. However, high levels of driving aggressiveness do not lead to a significant increase in energy consumption, even though almost the same amount of wheel work is required as for velocity modified driving behavior. This is due to the fact that only the inertia work part of wheel work increases and so does the amount of energy recuperated by regenerative braking.

Bibliography

[1] Arfa Grunditz, E. ; Thiringer, T. : Characterizing BEV Powertrain Energy Consumption, Efficiency, and Range During Official and Drive Cycles From Gothenburg, Sweden. In: *IEEE Transactions on Vehicular Technology* 65 (2016), Jun, Nr. 6, 3964–3980. http://dx.doi.org/10.1109/tvt.2015.2492239. – DOI 10.1109/tvt.2015.2492239

[2] Berry, I. : *The Effects of Driving Style and Vehicle Performance on the Real-World Fuel Consumption of U.S. Light-Duty Vehicles*. Massachusetts Institute of Technology, 2010

[3] Chen, H. ; Gao, B. : *Nonlinear Estimation and Control of Automotive Drivetrains* -. Berlin Heidelberg : Springer Science and Business Media, 2013. – ISBN 978–3–642–41572–2

[4] Gang, L. ; Zhi, Y. : Energy saving control based on motor efficiency map for electric vehicleswith four-wheel independently driven in-wheel motors. In: *Advances in Mechanical Engineering* 10 (2018), Aug, Nr. 8, 168781401879306. http://dx.doi.org/10.1177/1687814018793064. – DOI 10.1177/1687814018793064

[5] Giakoumis, E. G.: *Driving and Engine Cycles* -. Berlin, Heidelberg : Springer, 2016. – ISBN 978–3–319–49034–2

[6] Grauers, A. ; Sarasini, S. ; Karlström, M. : *Systems Perspectrives on Electromobility; Chapter 2: Why electromobility and what is it.* – ISBN 978–91–88041–07–4

[7] Grunditz, E. : *BEV Powertrain Component Sizing With Respect to Performance, Energy Consumption and Driving Patterns*. Chalmers University of Technology, 2014

[8] Guzzella, L. ; Sciarretta, A. : *Vehicle Propulsion Systems - Introduction to Modeling and Optimization*. Berlin Heidelberg : Springer Science and Business Media, 2012. – ISBN 978–3–642–35913–2

[9] Huertas, J. ; Giraldo, M. ; Quirama, L. ; Díaz, J. : Driving Cycles Based on Fuel Consumption. In: *Energies* 11 (2018), Nov, Nr. 11, 3064. http://dx.doi.org/10.3390/en11113064. – DOI 10.3390/en11113064

[10] Mario, V. ; Oriana, B. ; Peter, V. : Auxiliary systems consumption in electric vehicle. In: *Przeglad Elektrotechniczny* (2014), Nr. 12/2014, 172–175. http://dx.doi.org/10.12915/pe.2014.12.42. – DOI 10.12915/pe.2014.12.42. – ISSN 0033–2097

[11] Sharer, P. ; Leydier, R. ; Rousseau, A. : Impact of Drive Cycle Aggressiveness and Speed on HEVs Fuel Consumption Sensitivity. In: *SAE International, Warrendale, PA, USA, SAE Tech.* , Nr. 2007-01-0281, 2007.

[12] Sun, Z. ; Wen, Z. ; Zhao, X. ; Yang, Y. ; Li, S. : Real-World Driving Cycles Adaptability of Electric Vehicles. In: *World Electric Vehicle Journal* 11 (2020), Mar, Nr. 1, 19. http://dx.doi.org/10.3390/wevj11010019. – DOI 10.3390/wevj11010019

[13] Zhicheng, S. ; Boya, Z. ; Tianlu, D. ; Qingyu, M. ; Zhichao, L. ; Yaozong, X. ; Su, L. : Factors Affecting the Accuracy of Estimation of BEV Cruising Range. In: *IOP Conference Series: Materials Science and Engineering* 727 (2020), Jan, 012019. http://dx.doi.org/10.1088/1757-899x/727/1/012019. – DOI 10.1088/1757–899x/727/1/012019

A

Appendix 1

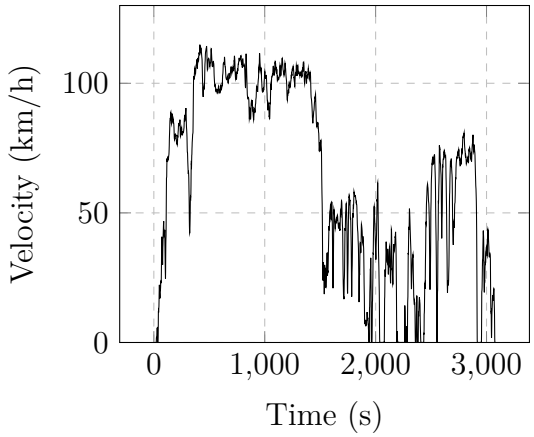

(a) HighSpeed 1 AtoB

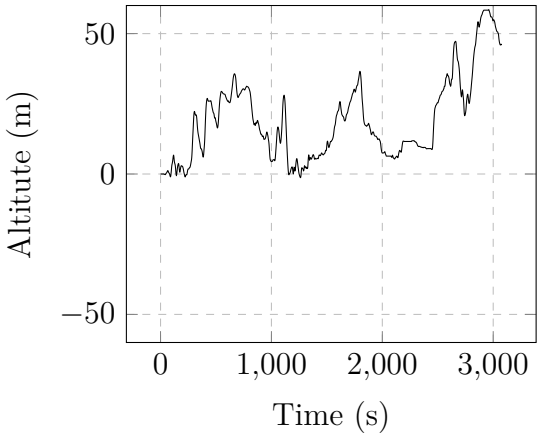

(b) HighSpeed 1 AtoB

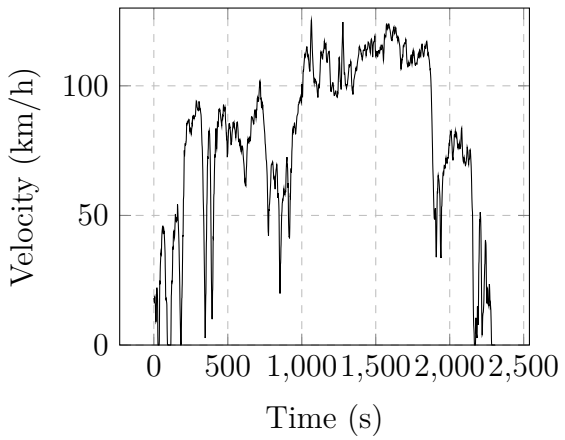

(a) HighSpeed 1 BtoA

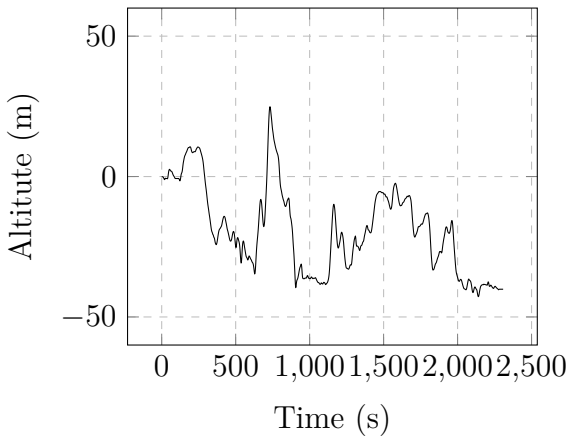

(b) HighSpeed 1 BtoA

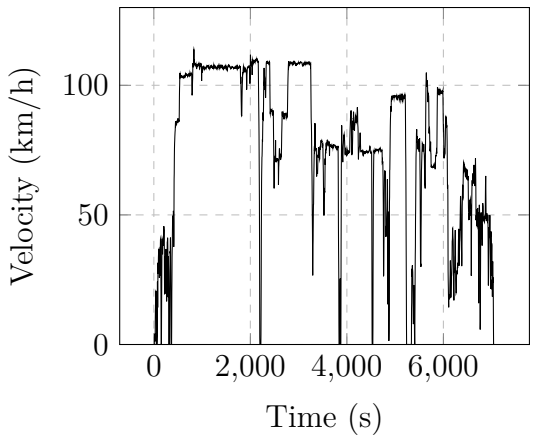

(a) HighSpeed 2 AtoB

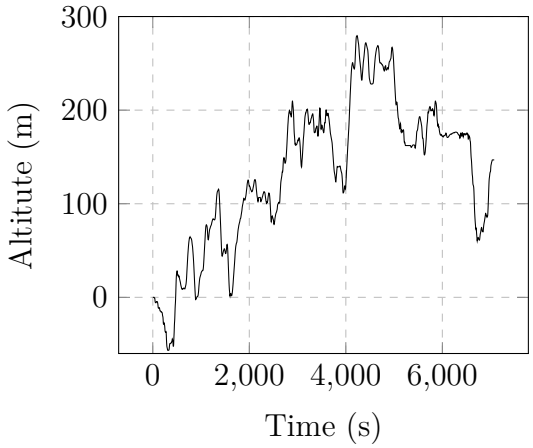

(b) HighSpeed 2 AtoB

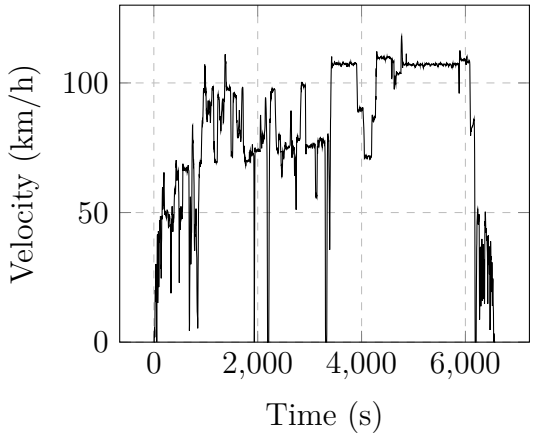

(a) HighSpeed 2 BtoA

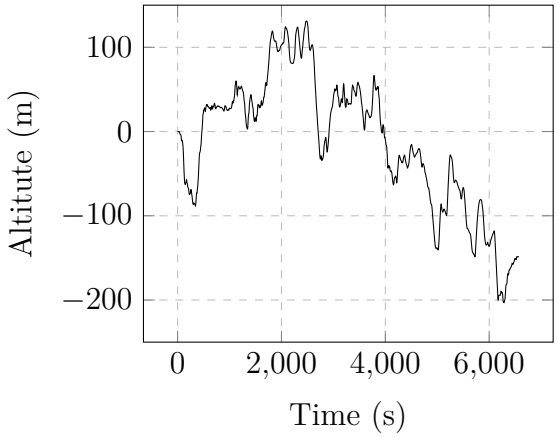

(b) HighSpeed 2 BtoA

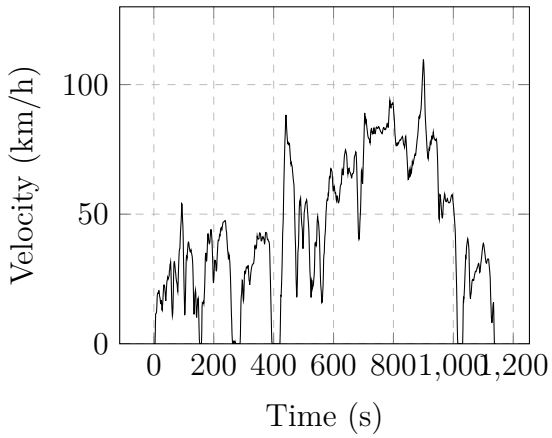

(a) MiddleSpeed 1 AtoB

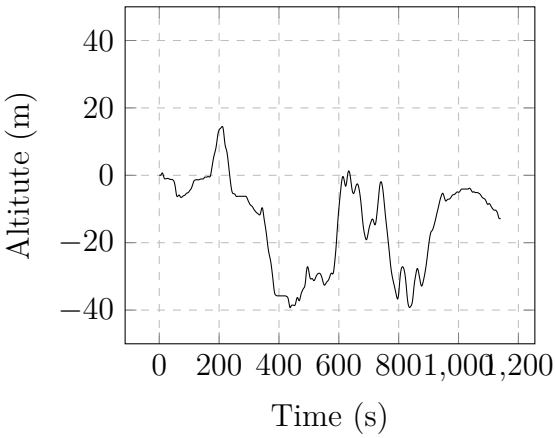

(b) MiddleSpeed 1 AtoB

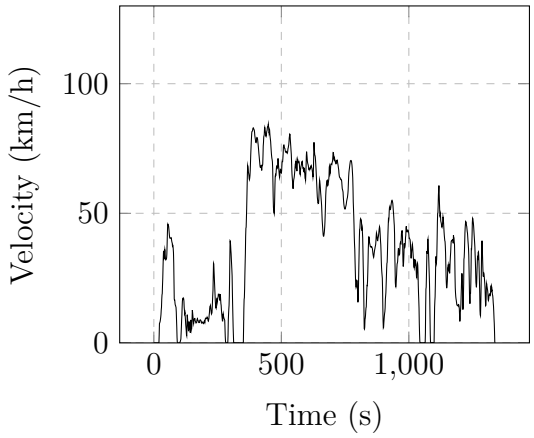

(a) MiddleSpeed 1 BtoA

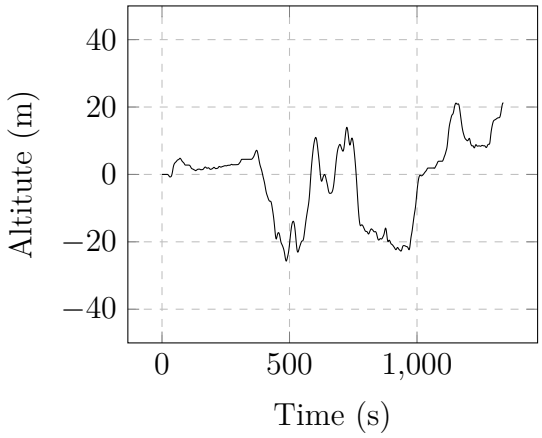

(b) MiddleSpeed 1 BtoA

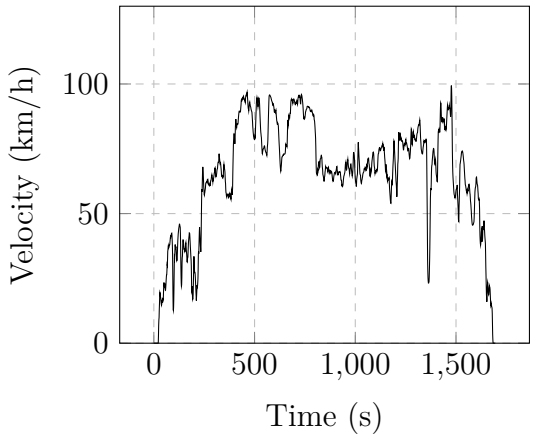

(a) MiddleSpeed 2 AtoB

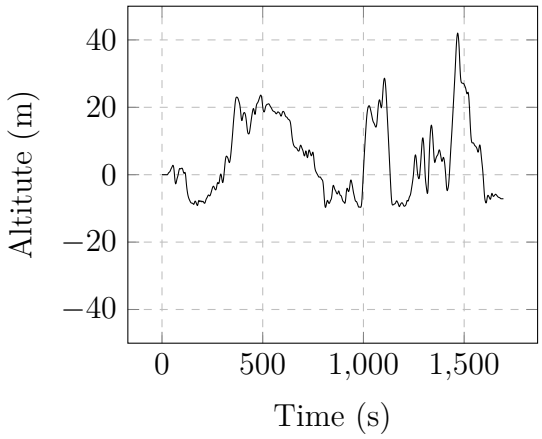

(b) MiddleSpeed 2 AtoB

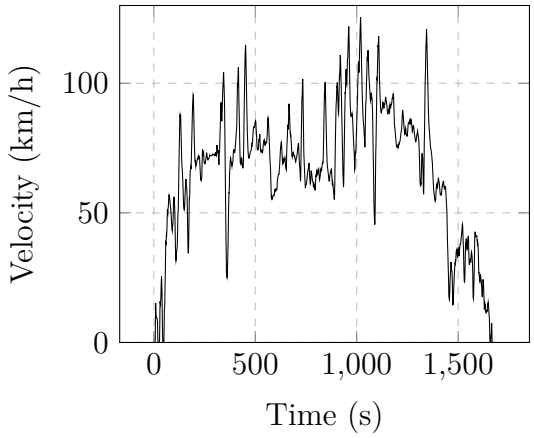

(a) MiddleSpeed 2 BtoA

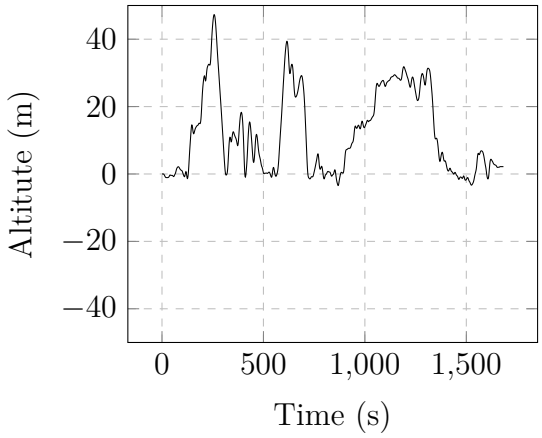

(b) MiddleSpeed 2 BtoA

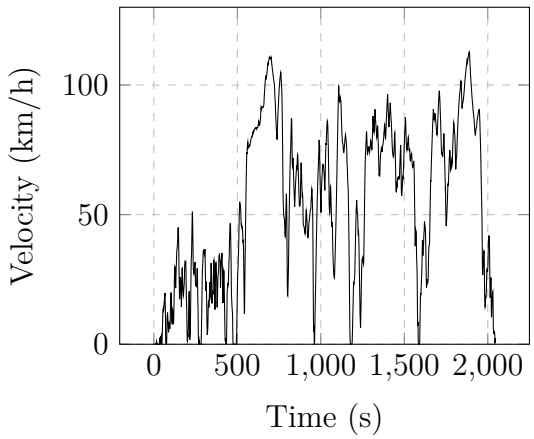

(a) MiddleSpeed 3

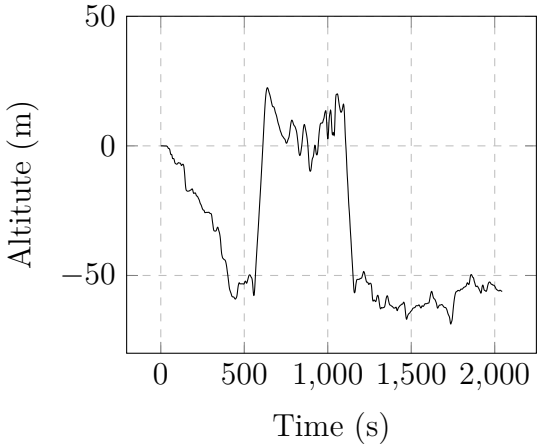

(b) MiddleSpeed 3

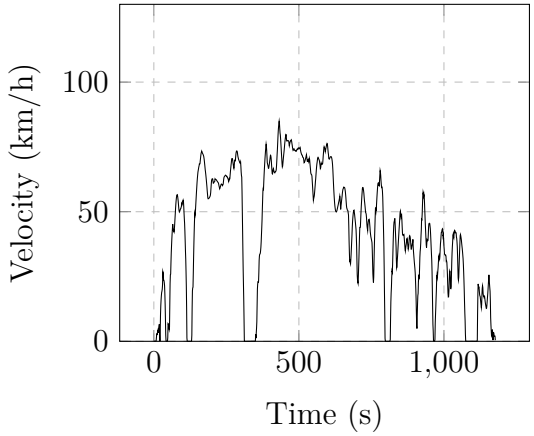

(a) MiddleSpeed 4

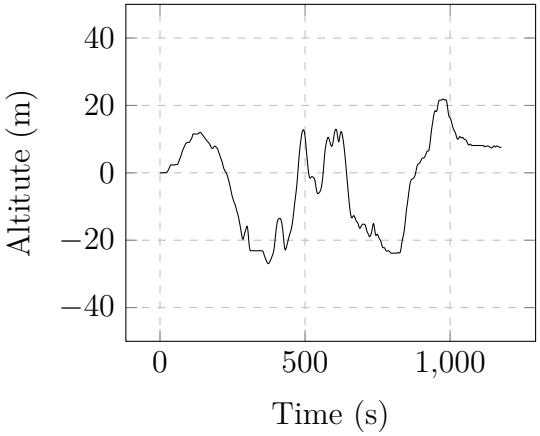

(b) MiddleSpeed 4

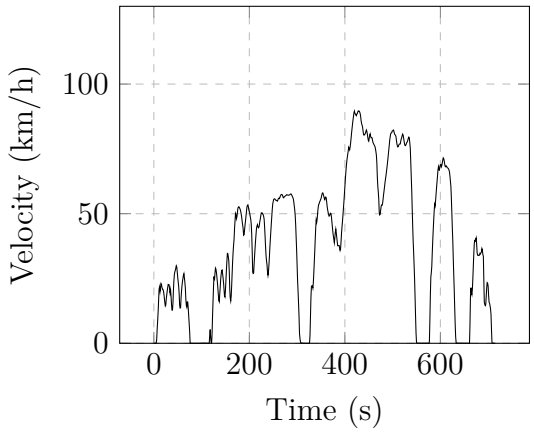

(a) MiddleSpeed 5a

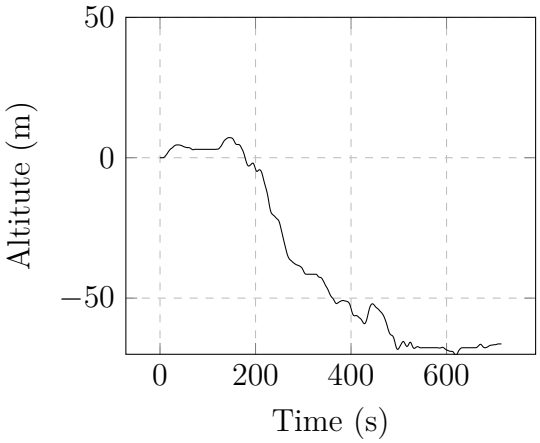

(b) MiddleSpeed 5a

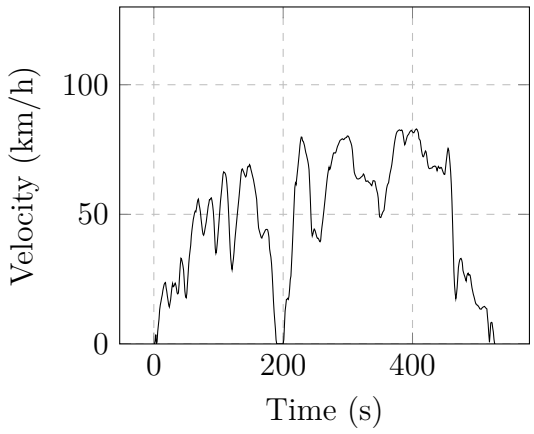

(a) MiddleSpeed 5b

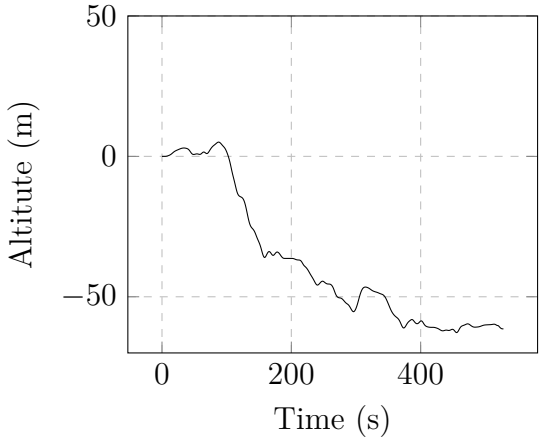

(b) MiddleSpeed 5b

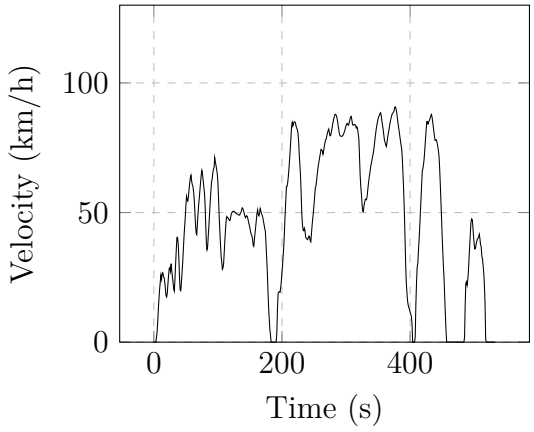

(a) MiddleSpeed 5c

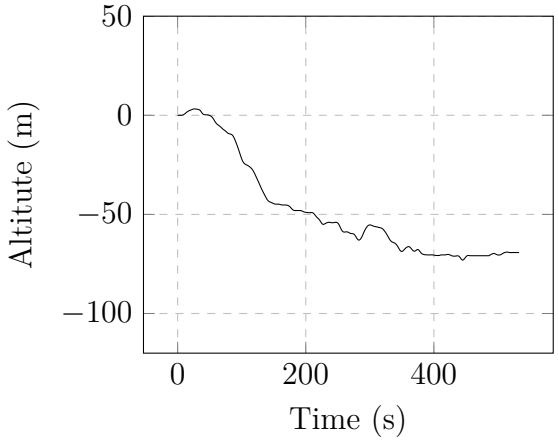

(b) MiddleSpeed 5c

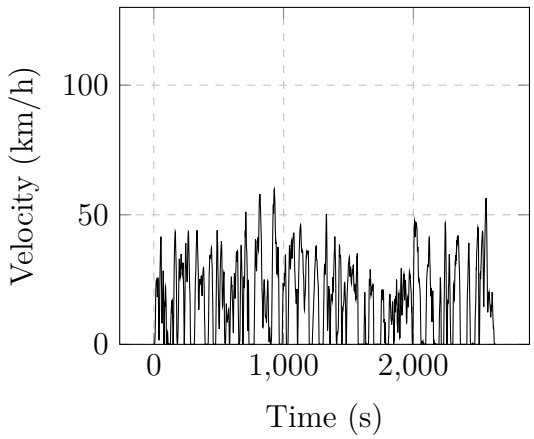

(a) LowSpeed 1

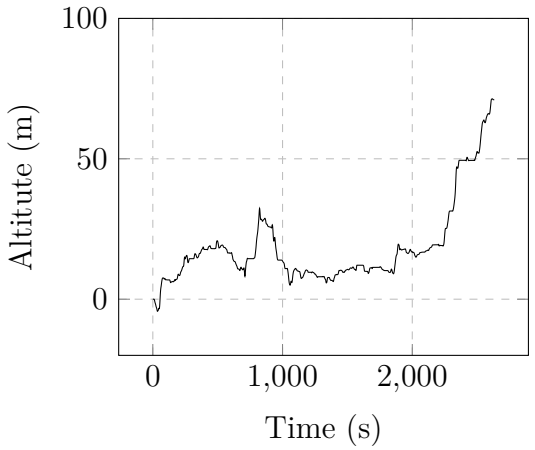

(b) LowSpeed 1

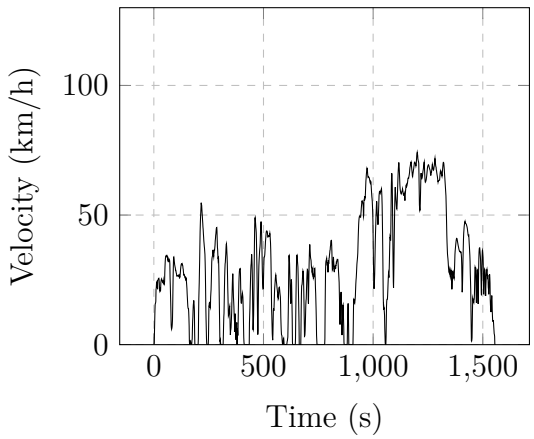

(a) LowSpeed 2

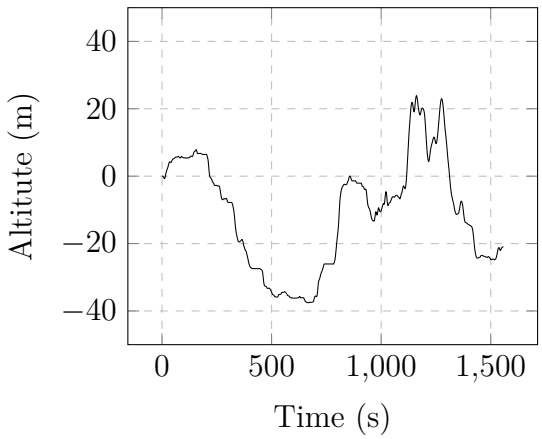

(b) LowSpeed 2

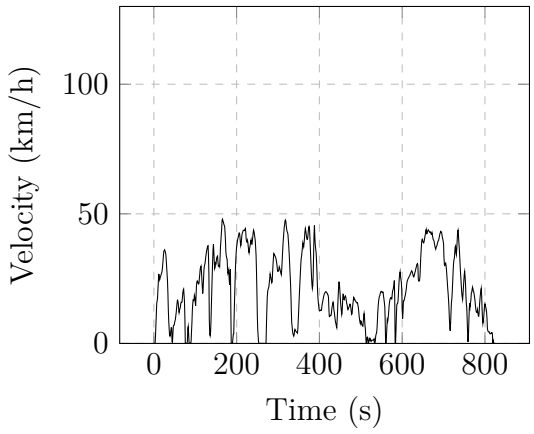

(a) LowSpeed 3

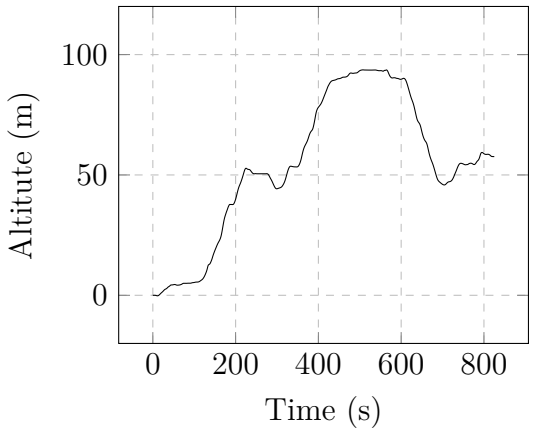

(b) LowSpeed 3

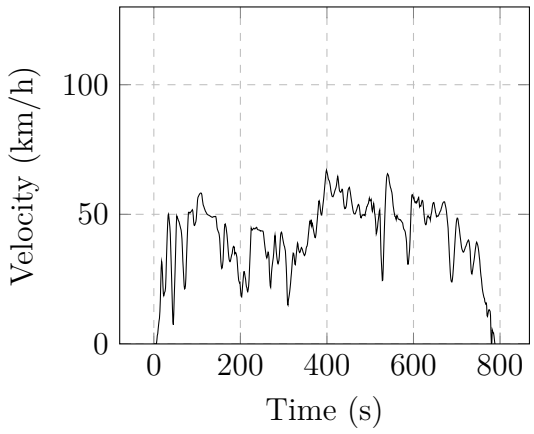

(a) LowSpeed 4 AtoB

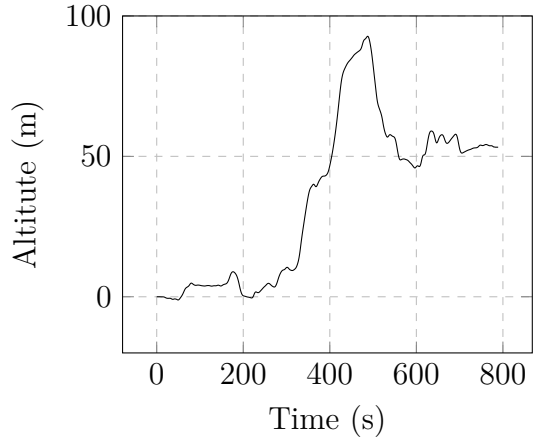

(b) LowSpeed 4 AtoB

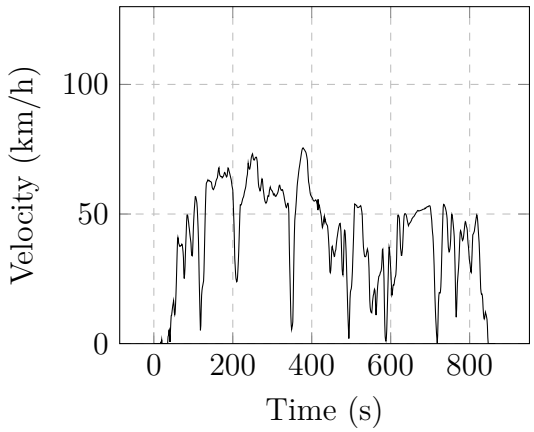

(a) LowSpeed 4 BtoA

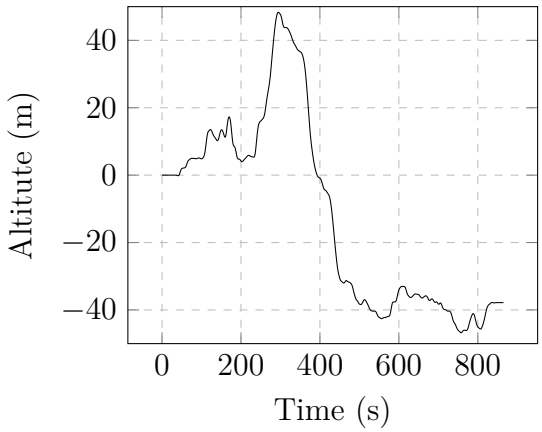

(b) LowSpeed 4 BtoA

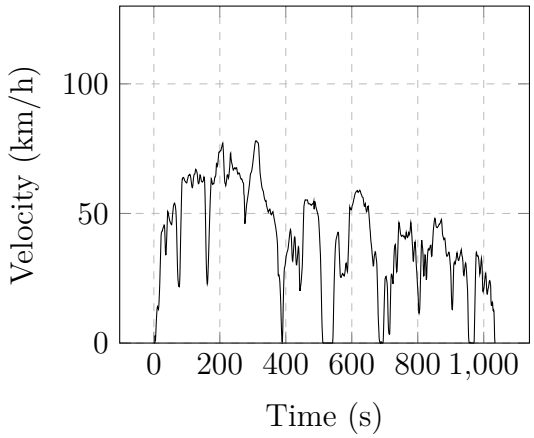

(a) LowSpeed 5

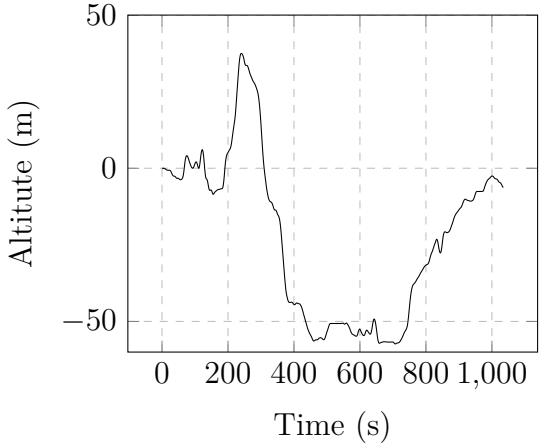

(b) LowSpeed 5

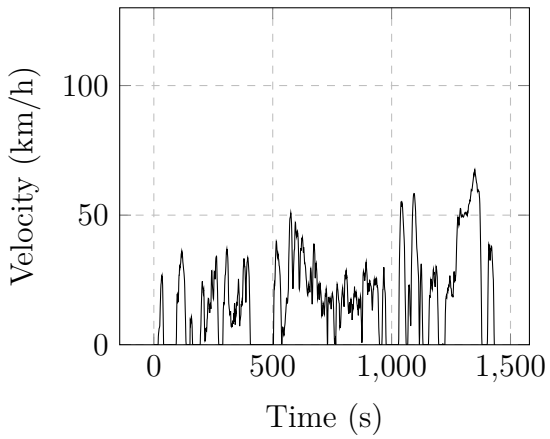

(a) LowSpeed 6

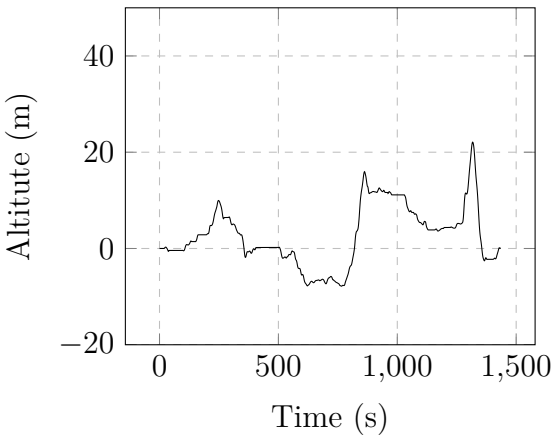

(b) LowSpeed 6

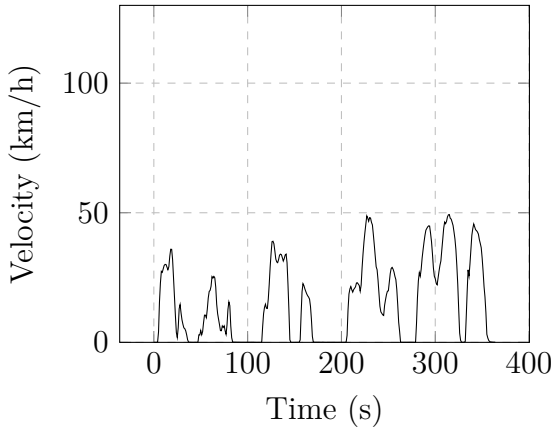

(a) LowSpeed 7

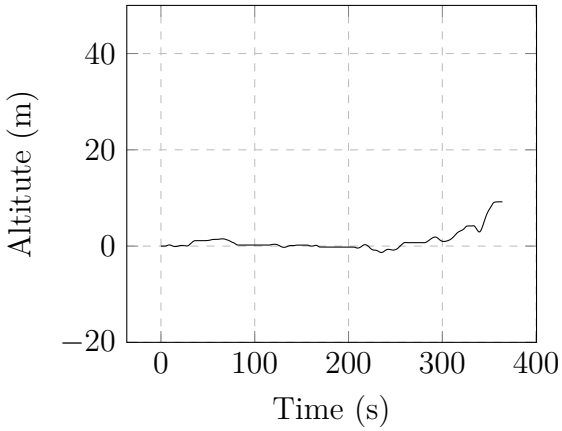

(b) LowSpeed 7

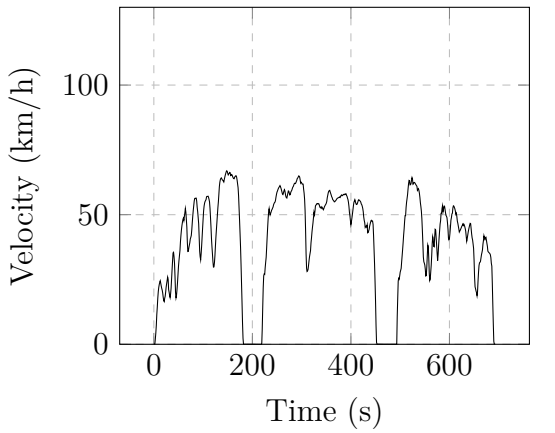

(a) LowSpeed 8 AtoB

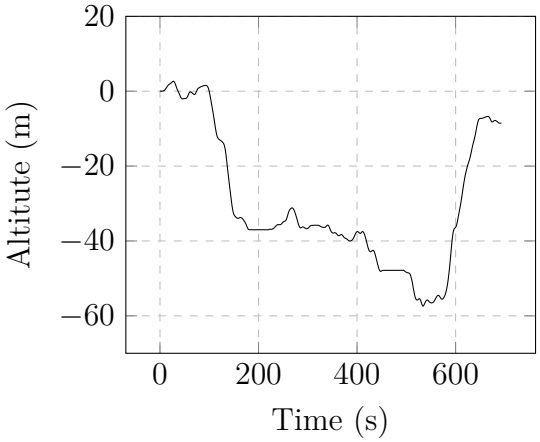

(b) LowSpeed 8 AtoB

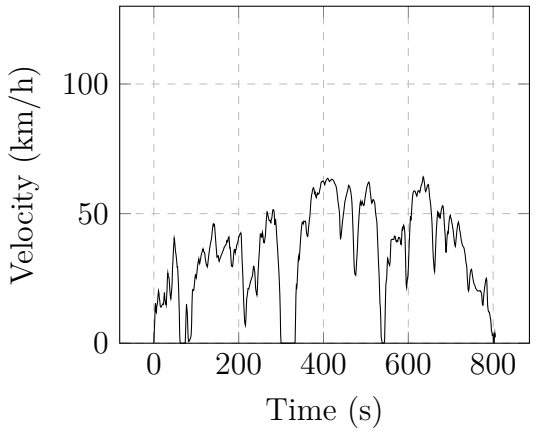

(a) LowSpeed 8 BtoA

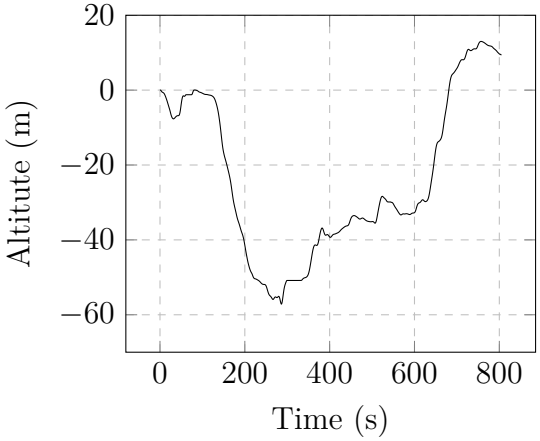

(b) LowSpeed 8 BtoA

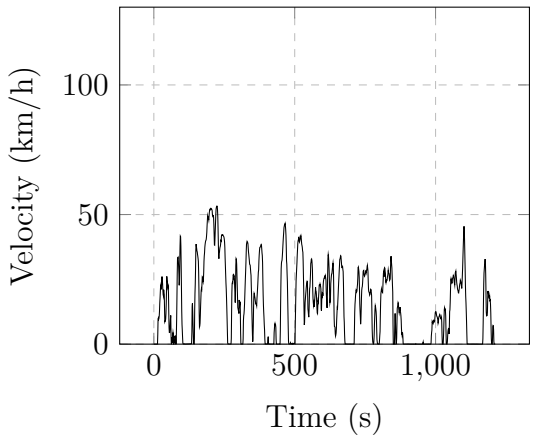

(a) LowSpeed 9

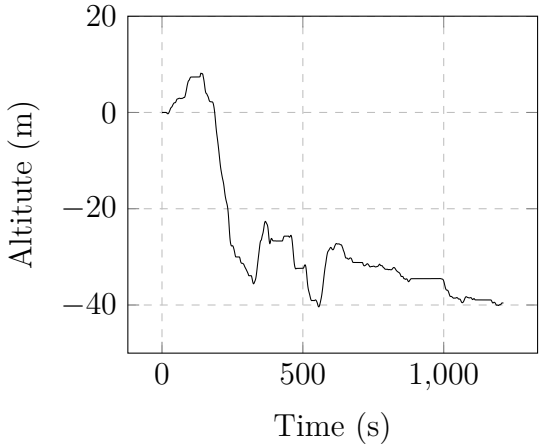

(b) LowSpeed 9